Targeting Canonical and Noncanonical Hedgehog Signaling Pathways in Cancer

by
Andrew R. Larsen

A dissertation submitted to Johns Hopkins University in conformity with the requirements for the degree of Doctor of Philosophy

Baltimore, Maryland
March, 2014

Abstract

The hedgehog (Hh) signaling pathway is activated in many types of cancer and therefore presents an attractive target for new anticancer agents. In the studies described here I demonstrate how mebendazole (MBZ), a benzimidazole with a long history of safe use against nematode infestations and hydatid disease, potently inhibited Hh signaling and slowed the growth of Hh-driven human medulloblastoma cells at clinically attainable concentrations. As an antiparasitic, MBZ avidly binds nematode tubulin and causes inhibition of intestinal microtubule synthesis. In human cells, MBZ suppressed the formation of the primary cilium, a microtubule-based organelle that functions as a signaling hub for Hh pathway activation. The inhibition of Hh signaling by MBZ was unaffected by mutants in the gene that encodes the Hh pathway signaling protein SMO, which are selectively propagated in cell clones that survive treatment with the Hh inhibitor vismodegib. Combination of FDA approved Hh inhibitor vismodegib and MBZ resulted in additive Hh signaling inhibition. Because MBZ can be safely administered to adults and children at high doses over extended time periods, I propose that MBZ could be rapidly repurposed and clinically tested as a prospective therapeutic agent for the many tumors that are dependent on Hh signaling.

One important genetic regulator of Hedgehog signaling is the tumor suppressor PTCH1. In addition to my studies of the canonical Hedgehog pathway and its inhibition by MBZ, I have also investigated a non-canonical pathway mediated by a novel PTCH1 homolog recently identified in our lab. I present evidence that this new gene, *PTCH53,* functions both in the canonical Hedgehog pathway and in a noncanonical Hh pathway that links p53 with innate immunity.

Readers

Fred Bunz, M.D., Ph.D.

Gregory J. Riggins, M.D., Ph.D.

Dissertation Committee

Fred Bunz, M.D., Ph.D. (Principal Advisor)

Gregory J. Riggins, M.D., Ph.D. (Chair)

Charles M. Rudin, M.D., Ph.D.

Acknowledgements

First and foremost I would like to thank my thesis advisor and one of the nicest people I have ever met, Fred Bunz. During my stay in his lab, Fred has gone above and beyond the standard expectation of a mentor. In science, assays are not always dependable, but Fred's optimism was. Even through the chaos of having two new children, he made sure that he was always accessible. His door was always open whether to discuss data, whether good or bad, or new experiments, whether good or bad. Fred guidance helped keep me on track and taught me to see the bigger picture through that data. I would never have graduated in such a short time frame if it wasn't for Fred teaching me how to utilize the tools around me. He communicated efficiency on a large scale. Rather than waste months trying to optimize assays relating to a tertiary question, he taught me to leverage the labs strengths to answers as many key questions with the least amount of work. It is a difficult position as a graduate transfer student, but I never felt any source of judgment from Fred over the years, only an enthusiasm for science.

My lab mate Jon Chung encouraged me to join Fred's lab after our first meeting, a piece of advice I am truly grateful for. Over the years Jon has helped with countless assays and experiments. His contributions to helping me become a better scientist were daily and included everything from optimizing westerns to long drawn out discussions about what direction scientific fields are headed in. It was a pleasure to work with such a diligent and brilliant scientist, and I hope one day to achieve a fraction of his organizational skills.

I would like to thank Greg Riggins for being a tremendously helpful and supportive collaborator and the chair of my committee. Greg lives over an hour away

from Hopkins, so when I had to schedule a committee meeting for 8 am in the morning I was shocked when Greg agreed to attend and downright amazed when he showed up on time. It is rare to see such selfless PI and I am lucky for being given the opportunity to collaborate with him. I thank Charles Rudin for serving on my committee even when it wasn't expected after moving his lab from Johns Hopkins to Sloan Kettering. I would also like to thank Ren-Yuan Bai of the Riggins group for both his expertise in mebendazole and helping me with all of my xenograph implantations.

I would like to thank all the members of the Radiation Oncology department for their useful feedback to my project over the years. I would also like to thank the division of neurobiology and all of its members for their support and aid in training of me as a scientist, especially the mentoring I received from both Russell Margolis and Fredrick Nucifora Jr.

Thank you to Johns Hopkins School of Medicine and the Cellular and Molecular Medicine Program. Thank you to Colleen Graham, Leslie Lichter, Rajni Rao and Robert Casero. I would have never made it here you hadn't given me a chance in the first place. Also, thank you to all my classmates; I don't think I would've made it to the good times without your support during the bad.

I thank my family for all of their never ending love and support. Throughout my entire life I knew that they would always support my decisions, no matter what I path I choose, as long as I was going after something that made me happy. I would like to thank my brother, James, for always finding time to see me on extremely short notices whenever I was in New York City, despite having the busiest schedules of any man I know. I would like to thank my parents for their years of patience and guidance. My

father has always instilled in me the wisdom that the one thing no one can take away from you is education. Thus, he taught me at a young age to invest my energy in bettering myself and the world that surrounds me. I would not of had the courage to take on the intimidating feat of a PhD without my family as an inspiration.

And finally, I would like to thank Sasha Borodovsky. She is more than just my significant other, she is also my best friend and a brilliant mind I am proud to call my scientific peer. I thank her for her relentless support in all my pursuits over the years. Whether it was a scientific project I was interested in or a new hobby, she not only supported my passions but drove me to excel at them. Every single one of my experiences during my time at Hopkins has been enriched by her presence and the future only excites me as I imagine all of the memories we will continue to create on our journey together.

TABLE OF CONTENTS

LIST OF TABLE AND FIGURES

Chapter 1: Background and relevant literature

1.1. Introduction

Activation of the hedgehog (Hh) signaling pathway is required for developmental morphogenesis and is frequently observed in human cancers (1, 2). Canonical Hh signals are initiated by the interaction of Hh ligands with the receptor PTCH1. In the unbound state, PTCH1 prevents SMO activation in the primary cilium, an organelle required for the transduction of various chemical and mechanical signals (3). In the presence of ligand, PTCH1 disappears from the cilium and SMO activates downstream effectors, including the GLI family of transcription factors (4). Several types of cancer, including basal cell carcinoma and medulloblastoma, are frequently caused by germline or somatic mutations in *PTCH1* or by less common alterations within the pathway that lead to constitutive signaling by SMO (1, 2). Alternative modes of Hh pathway activation in some of the most common types of cancer are suggested by the widespread presence of Hh ligands and evidence of elevated GLI activity in many tumors that lack pathway-activating mutations (5, 6). Greater understanding and targeting of the canonical and noncanonical hedgehog pathways can lead to improved cancer therapies.

1.2. Canonical and noncanonical hedgehog pathway

1.2.1. Discovery

The Hh gene was first discovered in 1980 by Christiane Nusslein-Volhard and Eric Wieschaus in a screen of mutant *Drosophila* and was named after the distinctive embryonic cuticle patterning in mutant flies (7). Hh was subsequently found to be a

secreted ligand that mediates developmental patterning. Hh signaling is evolutionarily conserved between *Drosophila* and higher organisms including humans. The vertebrate homologs of Hh ligand were being identified in 1993 (8). In contrast to *Drosophila*, vertebrates express three separate isoforms of the Hh protein including Sonic hedgehog (Shh), Indian hedgehog (Ihh), and Desert hedgehog (Dhh) (9). Each form shows a unique spatial and temporal distribution patterns and modulates distinct cellular responses (10). The downstream signaling of the Hh pathway has evolved from the single downstream transcription factor Cubitus interruptus (Ci) found in *Drosophila* to several human homologs known as the Gli family of transcription factors (11). In humans, the Hh family of proteins has proven to be a key mediator both in embryonic development and maintenance of continuously renewing tissues including adult stem cells (12).

The Hh pathway has shown to have a diverse and complex role in multiple aspects of embryonic development. Hh ligands control cell survival, proliferation, fate, patterning, and differentiation (13). Embryonic cells that secrete Hh are distinct from the cells that respond to it (14). Hh-responsive cells can either be adjacent to or at a significant distance from the Hh-secreteing cells. Hh can regulate cell numbers and fate in the brain, spinal cord, limbs and in many internal organs including the heart (9). The importance of Hh ligands is highlighted by the defects that occur following alterations in the signaling pathway during development. Outcomes related to Hh pathway inhibition include brain, facial and other midline defects including cyclopia, microencephaly, holoprosencephaly, absent nose, or cleft pallet (15-17). The effect of Hh ligands on cell fate is often translated through differences in signal strength and duration which modulate the response. These processes take place in close association with the developmental

regulation of bone morphogenetic protein, parathyroid hormones and retinoid signaling (18-20).

Although the role of Hh signaling is diminished after embryonic development, a modest level of expression in adulthood is critical to the regulation of tissue homeostasis. Elevated Hh activity is observed in renewable adult tissues including gut epithelium, pulmonary epithelium, prostate epithelium, and exocrine pancreas. Hh activity is also reactivated at damaged sites requiring tissue repair (21, 22). Additionally, stem and progenitor cell maintenance in the brain, epithelia, prostate, lung and mammary glands is regulated by Hh (12).

The generation of functionally mature Hh ligand begins with cleavage of a precursor protein to expose the active signaling domain (HhNp). Cholesterol is then transferred to the C terminal domain of the Hh polypeptide, this modification drives the association of the Hh protein with the plasma membrane (23). In the final processing step, a palmitoyl moiety is added to the N terminus by acetylation from the Rasp enzyme (24). Once processing is completed, fully active Hh ligand can be secreted from the cell.

1.2.2. The canonical hedgehog signaling pathway

In the absence of activation by extracellular ligand, the Hh pathway is constitutively suppressed by the 12 spanning transmembrane protein Patched 1 (PTCH1). PTCH1 sequesters the seven transmembrane spanning protein Smoothened (SMO) that is responsible for activating all downstream signaling **(Fig 1.1.)**. SMO is a functional G-protein-coupled receptor (GPCR) that aggregates around the primary cilia and whose activation is in part regulated by phosphorylation (25). The Hh signaling cascade is initiated by the binding of sonic hedgehog (Shh) ligand to PTCH1 on the cell

surface. This binding induces internalization of the bound proteins and degradation by lysosomes. Once de-repressed, SMO is able to dissociate the complex of suppressor of fused (SUFU) and glioma associated oncogene homologue (GLI) complex. The GLI family of zinc finger transcription factors includes GLI1 and GLI2 that are typically activators of the Hh pathway and GLI3 that is classically a repressor and is only active when Hh is unbound. When SMO is active the GLI complex undergoes nuclear translocation and regulates a large set of target genes.

Hh pathway activation results in increased expression of GLI1, GLI2, and PTCH1 transcripts and proteins. GLI1 transcripts are a useful readout of pathway activity and are frequently used as a quantitative marker for Hh pathway activation in cancers. A variety of feedback loops tightly control duration and amplitude of the Hh response, which is why both suppressors (PTCH1) and activators (GLI1, GLI2) of the pathway are transcriptionally upregulated. Other downstream genes activated by Hh classically fall into three categories: suppressors of apoptosis (eg. BCL-2), promoters of angiogenesis (eg. angiopoietin-1, angiopoietin-2, n-myc, BMI1, VEGF), and promoters of metastasis (upregulation of Snail and suppression of E-cadeherin), but these are cell type dependent (17, 26-28). The canonical Hh pathway has proven to be an incredibly important for both development and homeostasis of progenitor cells in adulthood. The canonical pathway is defined as all of the processes that are regulated through the transcriptional activity of GLI family.

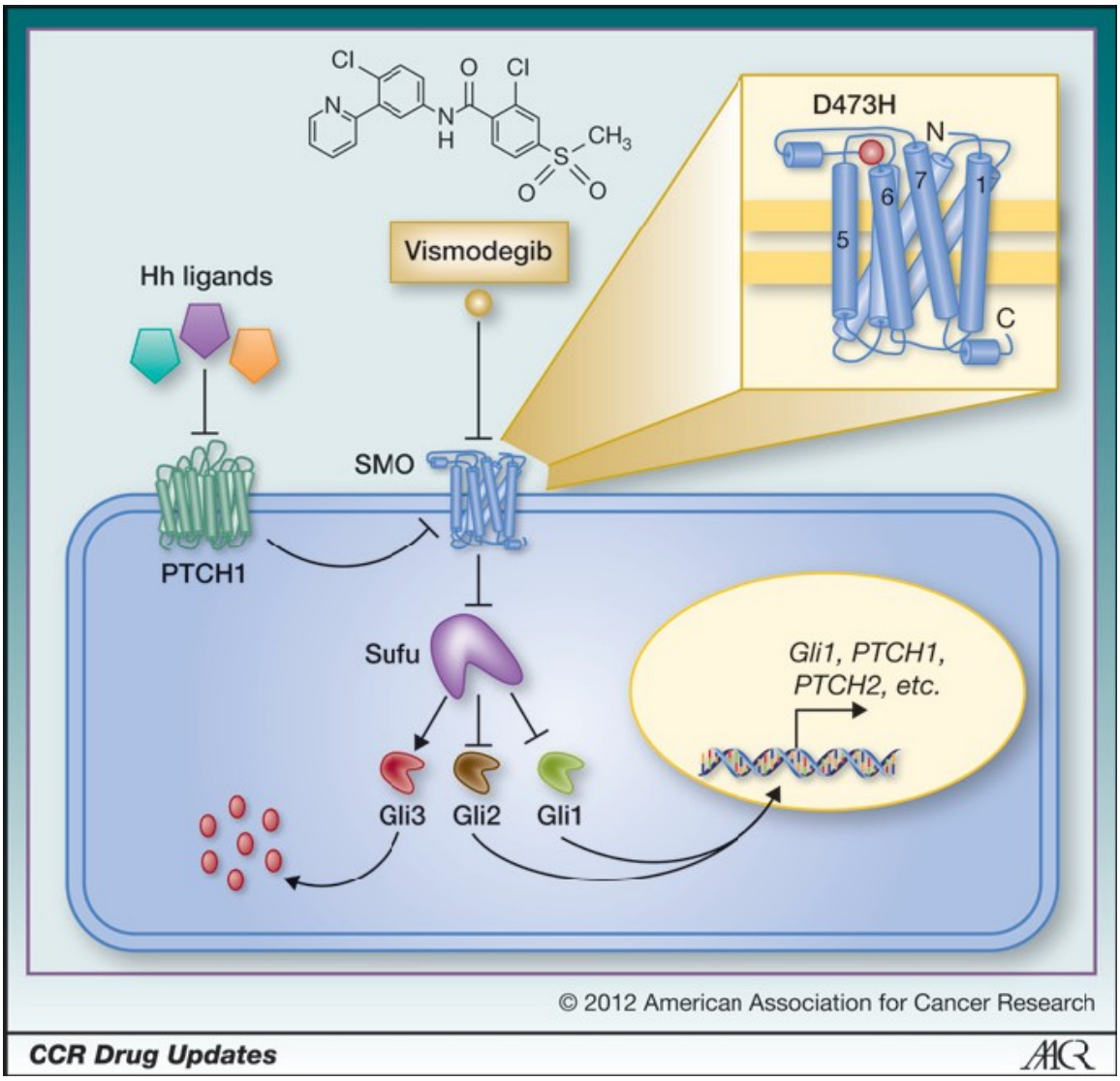

Figure 1.1. Hedgehog signaling (29)

The Hedgehog pathway is normally regulated through a cascade of primarily inhibitory signals. Depending on the tissue and developmental stage, one of 3 mammalian Hedgehog (Hh) ligands (Sonic Hh, Indian Hh, or Desert Hh) binds to cell surface PTCH1. Ligand binding to PTCH1 relieves PTCH1 inhibition of the critical activator of Hedgehog signaling, SMO. PTCH1 deficiency, found in the majority of BCC and about 30% of medulloblastoma, is associated with constitutive, ligand-independent activation of SMO. In mammalian cells, de-repression of SMO is associated with its translocation

from internal vesicles to the cell membrane cilium (not shown). Active SMO signals downstream through an intermediary Sufu, promoting the release of Gli family transcription factors, which can then translocate to the nucleus to affect gene transcription. There are multiple Gli proteins whose functions are somewhat cell type dependent; in general, Gli2 seems to be a particularly strong activator of downstream gene transcription (along with Gli1), while Gli3 is inhibitory in most contexts. Pathway activation and release from Sufu can lead to proteosomal degradation of Gli3 and to preferential nuclear translocation of Gli1 and Gli2, which activate transcription of multiple target genes, including key regulators of the Hedgehog pathway, notably Gli1 and PTCH1.

1.2.3. Primary cilia

Primary cilia are stationary microtubule based organelles that extend from the cell surface and mediate various extracellular signals to the cell through the intraflagellar transport system. Primary cilia, unlike the cilia of cells lining the human airway, are non-motile extensions from the plasma membrane. Primary cilia are expressed in vertebrates in various tissues. Their function is to detect changes in the extracellular environment. The primary cilium is the point of localization for signaling proteins in the Hh pathway, and is therefore considered the center for mediating most Hh signaling. Dysfunctional primary cilia have been linked to several human development disorders that resemble conditions caused by genetic defects in Hh signaling. For example, the human limb abnormality polydactyly has been linked to disrupted Hh signaling and also is seen in patients with Bardet-Biedl syndrome and Meckel-Gruber syndrome, both of which are characterized by defective ciliary function (30, 31).

The primary cilium is a dynamic organelle as it extends during interphase and is reabsorbed during cell cycle progression (32). This process is tightly linked to the cell cycle because the microtubule basal body that form the primary cilia's base contains centrioles that move away from the cell surface to a spindle pole during mitosis. During interphase, the extension of the primary cilium is initiated by centrioles moving to the plasma membrane and the aggregation of pericentriolar material around them. These structures promote microtubule polymerization (33). Tubulin polymerizes to form the core of the primary cilium, known as the ciliary axoneme. Between the ciliary axoneme and the basal body exist terminal plates, transition fibers, and condensed lipids. All of

these components are believed to contribute to the regulation of bidirectional protein trafficking between the cilia and the cytoplasm (34).

It is well understood that the major canonical hedgehog pathway components, PTCH1, SMO, SUFU, and GLI family of transcription factors, localize to primary cilia at various times (4, 35). The exact sequence of events following Hh activation remains to be definitively described.

The key regulatory feature of the canonical Hedgehog pathway is the negative regulation of SMO by PTCH1. Initially, it was believed that the inhibition of SMO by PTCH1 was a result of a direct physical interaction between the two proteins, but new data support a model in which PTCH1 regulates SMO activity via its ability to localize to the primary cilium. One theory suggests that PTCH1 resides in the primary cilia and excludes SMO until Hh binding activates a translocation of PTCH1 to the base of the primary cilia allowing SMO to enter and de-repressing SMO's ability activate downstream Hh signaling (36). PTCH1 may regulate SMO trafficking to and from the cilia by modulation of cholesterol levels within the cilium (37). Mutational analysis suggests that intraflagellar transport functions downstream of activated SMO and upstream of the Gli family of transcription factors, thereby defining the critical range in which primary cilia mediates Hh signaling (38). In support of this hypothesis, mice with mutations in basal body proteins Ofd1, Mks1, and Ftm exhibit abrogated cilia formation and these mutations also confer suppressed Hh signaling in response to ligand (39-41). Current evidence thus indicates that functional primary cilia are required for mediating competent downstream Hh pathway signaling.

1.2.4. Noncanonical hedgehog signaling pathways

A noncanonical Hh signaling pathway is a loose definition for any pathway that involves the upstream ligand and receptor components, but does not appear to involve downstream activation of the GLI proteins (42). Though poorly understood, these pathways have been proposed to fall into two distinct classes: a type 1 noncanonical pathway operates through *PTCH1* independently of the activity of *SMO* or *GLI*, while a type 2 pathway is mediated through *SMO* activity unrelated to *GLI* signaling (43).

Hh signaling suppresses apoptosis through multiple mechanisms that involve both canonical and noncanonical pathways. Canonical regulation of programmed cell death is controlled by GLI-mediated expression of pro-survival genes such as BCL-2 and activation of the survival kinase AKT (44, 45). In a poorly understood noncanonical pathway, *PTCH1* overexpression induces apoptosis that cannot be rescued by overexpression of *SMO*, while *PTCH1* knockdown increases cell survival (46, 47). Direct regulation of apoptosis by *PTCH1* is mediated through its C-terminal domain.

Canonical Hh signaling has shown to be an important driver of proliferation by through expression of *n-myc* and *cyclin D1* (48, 49). However, in the absence of Shh ligand, PTCH1 binds to phosphorylated Cyclin B1 and inhibits mitosis in a noncanonical fashion (50).

Type 2 noncanonical signaling is by definition mediated through SMO, independently of downstream GLI1. When stimulated by Hh ligand, SMO activates both GTPase RhoA and Rac1 by releasing Tiam1 that it normally sequesters (51). SMO's activation of RhoA causes the immediate formation of actin stress fibers within minutes and tubulogenesis within hours (52). *SMO* knockout cell lines are incapable of activation of RhoA and Rac1 and fibroblast migration is only possible in cells with functional

SMO (53). Shh ligand can also activate several Src family kinase to regulate axon guidance through SMO. Studies have shown Shh stimulated cell migration and cytoskeletal rearrangements are mediated through SMOs upregulation of the arachidonic acid metabolite leukotriene that induces lamellipodia formation and neurite projections (54, 55).

1.2.5. Adult progenitor and stem cells

The formation and maintenance of adult hematopoietic stem cells relies on the presence of Hh signaling. Accordingly, both hematopoiesis and vasculogenesis are inhibited in mouse embryos that lack Hh signaling (56). Similar to development, each of the three isoforms of Hh has a functionally unique role in adult progenitor cell homeostasis. In stromal cells after a bone marrow transplant, hematopoeitic regeneration is dependent upon Ihh overexpression (57). Expansion of primitive hematopoietic stem cells can be successfully achieved by activation of the Hh pathway (58).

Hh ligands control the proliferation, specification, and differentiation of embryonic neural precursors, and are required for the maintenance of adult quiescent neural stem cells. A well-defined role of Shh in differentiation is its expression from Purkinje cells during cerebellar development, during which ligand induces the rapid proliferation of granule cell precursors (59).

Deregulation of the Hh pathway within stem cell niches has been shown to contribute to a diverse range of cancers and disorders including Gorlin syndrome and Greig cephalopolysyndactyly syndrome (60). A hallmark of these cancers is the activation of the pathway without the presence of any Hh ligand. However, other

cancers appear to exhibit ligand dependency including gastrointestinal tumors, gliomas, hematological malignancies and prostate cancer (5, 21, 61, 62).

1.3. Hedgehog and cancer

1.3.1. Basal cell carcinoma and nevoid basal cell carcinoma

Basal cell carcinomas (BCC) represent a third of all cancers diagnosed every year in America, with a lifetime risk of 1 in 6 overall and 1 in 3 for Caucasians (63). Nearly all sporadic BCC are driven by aberrant Hh signaling (64). 90% of cases are driven by inactivating mutations of the Hh pathway inhibitor *PTCH1* and the other 10% are driven by activating mutations in the Hh pathway activator *SMO*. Furthermore, loss of p53 promotes BCC development in part by increasing expression of *SMO* (65). This finding is supported by preclinical *in vivo* models where homozygous loss of *TP53* accelerates formation of medulloblastoma in $Ptch1^{+/-}$ mice (66).

Mutations that affect the Hh pathway also play a critical role in hereditary cancer. Nevoid basal cell carcinoma (NBCC), commonly known as Gorlin syndrome, is an autosomal dominant inherited disease that is characterized by multiple cutaneous basal cell carcinomas. Medulloblastoma or rhabdomyasaroma are also associated with this syndrome.(64). The disease is caused by inactivating mutations in the *PTCH1* gene rendering it unable to inhibit *SMO* (67). *In vivo* models for NBCC use mice with $Ptch1^{+/-}$ backgrounds and display multiple phenotypes representative of patients including a 25% occurrence of medulloblastoma (60, 68, 69). When $Ptch1^{+/-}$ mice are crossed with *Tp53* knockout mice the rate of tumor occurrence increases to 100% with significant acceleration if exposed to ionizing radiation (70).

1.3.2. Medulloblastoma

Medulloblastoma is the most common malignant brain tumor in children and the leading cancer mortality in children (71). There are four distinct molecular subgroups of medulloblastomas, defined by their mutational profile and patterns of gene expression. Group 1 medulloblastomas are driven by the Sonic Hedgehog (Shh) pathway and constitute about a third of diagnoses. These tumors typically respond relatively well to conventional treatment. The well-defined role of Shh signaling in cerebellar development and initiation of rapid granule cell precursor proliferation creates a clear link between Hh pathway activation and transformation of the granule cell precursors leading to medulloblastoma (72). Interestingly, there is a similar gene expression pattern in group 1 medulloblastomas and granule neuron progenitor cells (73). Oncogenesis is believed to occur when actived Hh pathway in granule neuron progenitor cells fails to become normally down-regulated during terminal cell differentiation. Of the group 1 category of medulloblastomas, half are associated with a loss or mutation of either PTCH1 or SUFU, or a gain of function SMO mutation, with PTCH1 inactivation being the most common (74). Thus, there is a subset of medulloblastomas that are exhibit Hh pathway overactivation without a representative Hh driver mutation, highlighting our incomplete characterization of the pathway.

1.3.3. A broad role for hedgehog pathway activation in human cancers

Many cancers exhibit evidence of activated canonical Hh signaling in the apparent absence of pathway mutations. *GLI1* overexpression has been identified in glioblastoma and childhood sarcoma (75, 76). and Shh ligand and elevated GLI expression have been detected in melanomas, lung cancers, ovarian cancers, adrenocortical cancers and colorectal cancers (5, 6, 77-80). Several cancers that do not appear to harbor Hh signaling mutations have shown sensitivity to SMO inhibitors in both *in vitro* and *in vivo* (81). In total, as many as 25% of all human tumors may depend on Hh pathway activity for growth (82). The hedgehog pathway can be activated by Shh ligand in both paracrine and autocrine dependent manners. SMO inhibitors showed a successful survival response in a pancreatic cancer mouse model along with depletion of tumor associated stromal tissue (83). In leukemia, GLI1 has been shown to function autonomously to promote cell survival and studies indicate it functions independently of Shh and SMO (84).

Several *in vitro* models are able to replicate Hh pathway activation usually only seen in patients or *in vivo*. The Hh pathway has been identified as a driver of proliferation in malignant pleural mesothelioma cells and as a key component for tumor maintenance in pancreatic cancer (85). Pancreatic cancer cells lines with pancreatic cancer stem markers ($CD133^+/CD44^+/CD24^+/ESA^+$) all have shown dependence on Hh pathway components (86).

1.4. A homolog of *PTCH1*

The human genome contains as many as 10 homologs of PTCH1. The roles of these genes in the regulation of the Hh pathway are unknown. Our laboratory recently identified a *PTCH1* homolog that is transcriptionally regulated by p53, and was accordingly designated *PTCH53* (**Fig 1.2.A**).

More than 50% of human tumors contain either a mutation of deletion of *TP53* (87). p53 is a major tumor suppressor that functions by regulating cell cycle and apoptosis (88). More than 500 p53 binding sites have been identified in the human genome, however the entirety of its tumor suppressor mechanism is yet to be identified (89). *PTCH53* transcription was dependent on functional *TP53* expression in a diverse range of human tumor types according to the global gene expression data of the cancer cell line encyclopedia.

Inducible overexpression and knockdown of *PTCH53* in immortalized human retinal pigment epithelial (hRPE1) cells showed a greater than two fold induction and suppression respectively of 15 interferon-stimulated genes typically activated by type 1 interferon **(Fig 1.2.B and 1.2.C)**. *PTCH53* plays a potential role in GLI suppression, but appears to be a significant regulator of interferon-stimulated genes. While the role of ligand in the process is unclear, it is possible that PTCH53 thus functions in a noncanonical pathway to mediate the interferon responses.

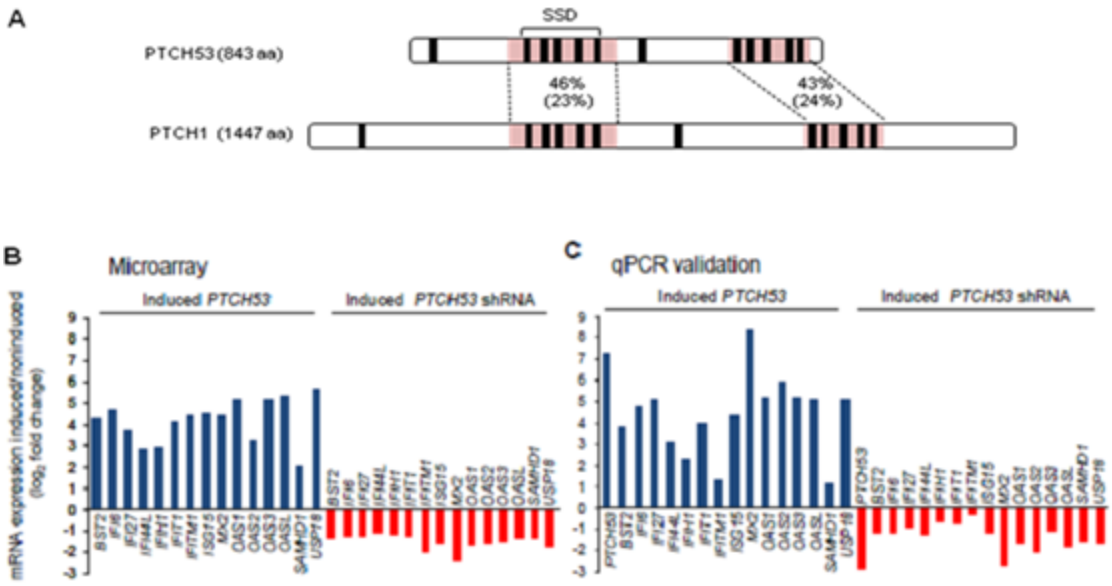

Figure 1.2. *PTCH53* regulates interferon stimulated genes (Jon Chung et al., unpublished)

(A) *PTCH53* expression is induced by p53. Predicted primary structure for PTCH53 and PTCH1. Black bars indicate transmembrane domains. SSD = sterol-sensing domain. The two regions of homology characteristic of Patched proteins are shaded in orange. The % similarity (% identity) within these regions is indicated. (B) Regulation of interferon stimulated genes by *PTCH53*. hTERT-RPE1 cells with doxycycline-inducible *PTCH53* cDNA or a doxycycline-inducible *PTCH53* shRNA were grown in low serum media for 48 h prior to induction with doxycycline for 48 h. RNA was collected before and after doxycycline treatment. *PTCH53* RNA expression was measured by qPCR. Individual genes and their changes in expression after doxycycline treatment are shown. (C) In an independent experiment that replicated the conditions for the microarray experiment, differential expression of the fifteen selected genes and *PTCH53* was validated by qPCR.

1.5. Hedgehog Inhibitors

1.5.1. Cyclopamine

Cyclopia is a birth defect characterized by an undivided forebrain and the absence of median facial structures. An endemic of cylopia occurred among the western United States in sheep herds during the 1950's (90, 91). The cause was determined to be consumption of *Veratrum californicum,* a lily indigenous to subalpine meadows. The lily contains the teratogenic steroidal alkaloid cyclopamine that was eventually proven to be a naturally occurring potent Hh inhibitor (92). This was a key finding as it proved that the Hh pathway contained druggable targets. The clinical applicability of Hh inhibition became apparent when cyclopamine was shown to reverse the oncogenic effect of both the inactivating mutation of *PTCH1* and the activating mutation in *SMO* (93).

Cyclopamine acts as a Hh antagonist by binding to the heptahelical bundle of SMO and thereby stabilizing the protein in an inactive conformation (94). Inhibition of SMO causes suppression of GLI transcriptional activity. Although it was proposed as a potential anticancer drug, cyclopamine never went to clinical trial for treatment of any Hh driven cancers due to its many off-target effects such as induction of neuronal-nitric oxide synthase and neutral sphingomyelin phosphodiesterase 3 (95). Instead, a cyclopamine derivative known as Saridegib or IPI-926 completed Phase 1 and went to a Phase II clinical trial, but was discontinued before completion due to lack of efficacy in 2012.

1.5.2. Vismodegib

In 2000, a growing body of evidence supported the role of Hh signaling in many cancers. The discovery that the small molecule cyclopamine could inhibit Hh signaling drove biotech and pharmaceutical companies to begin developing their own inhibitors. The first successful Hh antagonist brought to clinical trials in 2007 was vismodegib (GDC-0449) developed by Genentech. Vismodegib was structurally unrelated to cyclopamine, but shared the same effective strategy of binding to the extracellular domain of SMO in tumors with active Hh (96). However, vismodegib possessed a higher affinity and specificity to SMO than cyclopamine. This affinity was achieved through screening multiple candidates in an Hh reporter assay. In this assay, C3H10T1/2 mouse fibroblasts cells were transfected with Gli1-luciferase reporters and treated with media conditioned with ShhN, a truncated form of the Shh ligand bearing an identical amino acid sequence but lacking the cholesterol modification. Among the many compounds tested vismodegib resulted in a 20-fold increase in affinity compared to cyclopamine with an IC_{50} of 13 nM (the IC_{50} of cyclopamine is 300 nM) (97). In Hh-dependent medulloblastoma flank allografts generated from $Ptch^{+/-}$ mice, complete regression was achieved by vismodegib at doses as low as 12.5mg/kg *in vivo* .

Vismodegib (marketed as Erivedge) became the first SMO antagonist to be FDA approved for clinical use in 2012 in treatment of locally advanced and metastatic basal cell carcinomas (98). It is currently being tested for use in adults and children with many diverse types of tumors. There are currently 48 clinical trials involving vismodegib, the majority of which are ongoing. Many tumors are being tested, including medulloblastomas and gliomas, which are often refractory to conventional therapies (99).

Due to the unique inherited genetic driver of the NBCC, patients often aware of their disease prior to its first emergence or manifestation. The current standard of treatment is palliative care and includes repeated surgery to reduce tumor burden. Clinical trials are currently ongoing for attempting daily dosing of vismodegib as a preventative agent for these patients; however concerns of compliance have been raised due to its harsh side effects. Continuous treatment of low-toxicity Hh inhibitors has been proposed as a possible treatment for these patients in order to decrease chances of tumor emergence.

When used as a monotherapy, vismodegib is associated with adverse effects that include fatigue, vomiting, weight loss, decreased appetite, dysgeusia, dehydration, and muscle spasm (100). Such low-grade toxicities have contributed to treatment discontinuation and appear to be potentially problematic when vismodegib is combined with conventional agents (101). When used to treat a patient with metastatic medulloblastoma, vismodegib caused a response that was impressive but transient **(Fig 1.3)** (102). Genetic analysis of the vismodegib resistant subclones has shown they harbor SMO mutations (Smo D477G) that blocks vismodegib binding and subsequent Hh inhibition (103). Recurrent tumors that harbor a *SMO* mutation that confers drug resistance was also seen in a case report of BCC (103). Selection for *SMO*-mutant tumor cell populations can similarly be caused by vismodegib therapy in mouse models of medulloblastoma (103). Alternative strategies to inhibit Hh signaling have been explored for the prevention or treatment of such recurrent tumors (104).

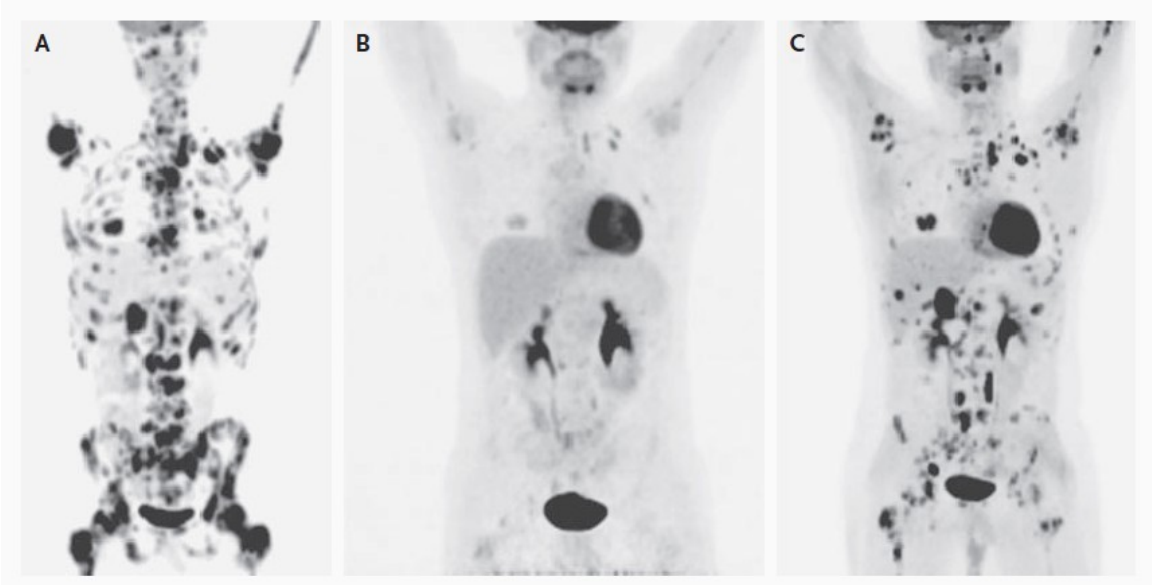

Figure 1.3. Transient response of a disseminated medulloblastoma to vismodegib treatment (102)

Whole-body projections from 18 F-fluorodeoxyglucose (FDG)–PET scans are shown. Panel A shows the pretreatment scan; Panel B, the repeat scan after 2 months of therapy with the hedgehog pathway inhibitor vismodegib; and Panel C, the repeat scan after 3 months of therapy, showing recurrent disease.

1.5.3. Itraconazole and Arsenic Trioxide

Drug development is both time and resource intensive with no guarantee of success. Even if a small molecule performs well in model systems, the chances of it maintaining its efficacy in patients without severe complications and completing clinical trials with FDA approval remains only 13% (105). The successful treatment of Hh driven cancers *in vitro* and *in vivo* by SMO inhibitors created a push to not only develop new Hh antagonists, but also to repurpose molecules that were already FDA approved. In 2006, James Kim screened 2,400 FDA approved or post-phase I trials drugs for efficacy against Hh signaling (106). The model used for screening had been previously established. ShhLight II cells are a mouse fibroblast cell line (3T3) with a stably integrated Gli-activated firefly luciferase (Gli-luc) reporter construct and a constitutive renilla luciferase (TK-renilla) reporter (93). The assay is performed by stimulating cells with Shh ligand to activate Gli transcription and measuring the increase in luciferase expression. The screen was designed to identify compounds that reduced luciferase activity, indicating inhibition of GLI transcription by Hh ligand. In evaluating therapeutic plausibility of all compounds identified by the screen, several factors were considered. These included whether the compound had previously received FDA approval for use in humans, whether Hh inhibition was could be observed at physiologically relevant serum concentrations, and whether the drug exhibited general toxicity. Of the 2,400 drugs screened by Dr. Kim's group, several showed activity against Hh at a dose range that was attainable in humans. One of these drugs was itraconazole, an FDA-approved, nontoxic drug that is a commonly prescribed antifungal, that can be administered systemically for months.

Itraconazole is a broad spectrum triazole antifungal used against *Aspergillosis, Candidiasis, Cryptococcosis, Blastomycosis, Sportotrichosis, Histoplasmosis*, and *Onychomycosis.* As an antifungal agent, the mechanism of action of itraconazole is inhibition of cytochrome P450 lanosterol 14-α-demeylase (14LDM). Itraconazole coordinates the heme Fe^{2+} in the active site of 14LDM. This coordination blocks the demethylation of lanosterols into ergosterols (107). In fungi, ergosterols perform the same basic function as cholesterol in mammals and are a critical component for cell membranes. A human homolog of 14LDM is critical for cholesterol synthesis; itraconazole has a preference for inhibiting the fungal form (108). However, high doses of itraconazole have shown to decrease cholesterol in humans (109). In ShhN-stimulated ShhLight II cells, itraconazole functions as a potent SMO antagonist with an IC_{50} of 800 nM. Interestingly, itraconazole acts on SMO at a distinct target site from cyclopamine and vismodegib. Follow up *in vivo* studies demonstrated that itraconazole could successfully inhibited growth of Hh-dependent flank models of medulloblastoma and BCC.

In addition to itraconazole, the screen by Kim et al. also identified several microtubule inhibitors. Vinblastine, vincristine, and paclitaxel were some of the vinca alkaloid derivatives that consistently performed as Hh antagonists at pharmacologically attainable concentrations. Cancers that respond to Hh antagonists typically require long courses of therapy (6, 110, 111). The microtubule inhibitors identified in the screen, while showing potential efficacy against the Hh pathway, were also potent mitosis inhibitors and were too toxic to be a considered long term therapy and therefore no further follow up studies were performed.

As of 2013, Arsenic trioxide (ATO) is the standard of treatment for concurrent chemotherapy of acute promyelocytic leukemia (APL), in addition to an approved combination therapy with all-trans retinoic acid (ATRA) against certain leukemias when unresponsive to first line therapies (112). The treatment carries significant risk due to known toxicities of arsenic poisoning, however its ability to induce apoptosis in cancerous cells under certain circumstances justify the treatment (113). While investigating ATO's effects, it was noted that pregnant mice treated with ATO had a number of embryonic development problems consistent with Hh inhibition such as improper axial skeleton and limb development. Using the same screening assay that was used to identify itraconazole, investigators found that ATO inhibited Hh signaling with an IC_{50} of 700 nM.

Unlike the first generation of Hh inhibitors, ATO does not target SMO. Instead, it inhibits trafficking of GLI2 to the primary cilia to suppress of Hh signaling (114). Like itraconazole, ATO suppressed growth *in vivo* against the flank Hh-driven medulloblastoma model.

ATO has been reported to have significant side effects. A quarter of patients undergoing APL induction therapy with ATO and/or ATRA will experience differentiation syndrome, a potentially fatal compilation caused by leukemic blasts undergoing cellular migration, endothelial activation, and release of interleukin and vascular factors (115). It is life threatening side effect that can lead to tissue damage and acute renal failure. ATO treatment can also induce a variety of heart related issues including atrioventricular block, QTc prolongation, and torsades de pointes-type arrhythmias (116). Other adverse effects from ATO treatment include peripheral

neuropathy, musculoskeletal pain, leukocytosis, and hepatitc toxicity (117). For these reasons, patients receiving ATO should be closely monitored.

Itraconazole and ATO can be combined for an additive effect against Hh signaling. Each drug, both independently and together, showed efficacy against all known vismodegib and cyclopamine resistant forms of SMO (104). While neither compound was able to completely suppress growth like vismodegib, they were able to both significant delay tumor growth alone and with greater efficacy together. Transcripts from the tumors were analyzed by qRT-PCR and showed that all Hh antagonists caused reduced GLI1 levels by at least 40%. As expected, the degree of GLI1 inhibition was found to correlate with treatment response in the medulloblastoma and BCC model. Lastly, all compounds and combinations were tested in an orthotopic Hh-driven vismodegib resistant (Smo^{D477G}) medulloblastoma. Only itraconazole and ATO showed efficacy and elicited a greater response in combination. This was the first evidence that both compounds could successfully pass the blood brain barrier.

While neither itraconazole nor ATO has the same efficacy of vismodegib against Hh driven cancers, they can contribute to an improved therapy by targeting separate components of the Hh pathway. While vismodegib resistant SMO mutations have emerged from treatment, combination therapy decreases the odds of a single clone with simultaneous compensatory mechanisms against both treatments. Therefore, simultaneously targeting both SMO and GLI2 transcription factor may provide an improved therapeutic response. Combination therapy involving vismodegib also provides the possibility of achieving the same amount of Hh inhibition while decreasing the vismodegib dosage to reduce unwanted side effects. However, both itraconazole and

ATO have their limitations. While clinical trials are ongoing for itraconazole, it has shown modest effect in castration-resistant prostate cancer and metastatic nonsquamous non-small-cell lung cancer. However, its effect on cancers in patients with clear Hh dependence has not yet been determined (118, 119). In addition, ATO has well characterized harmful side effects that need to be considered before pursuing as a therapy.

1.5.4. Drugs in the pipeline

As Hh pathway inhibition grows as a promising therapeutic strategy, novel inhibitors continue to be developed. Over 75 new inhibitors have been patented or are currently in the pipeline of various pharmaceutical companies (96). Although vismodegib is only FDA-approved for BCC, clinical trials are ongoing to test its efficacy in a variety of other of Hh-driven cancers. In addition, seven new Hh inhibitors have entered phase I and II clinical trials. The current Phase I or II clinical trial candidates includes IPI-926 (Infinity Pharm), LDE225 (Novartis), LEQ506 (Novartis), PF-04449913 (Pfizer), TAK-441 (Millennium Pharm), BMS833923 (Bristol Myers Squibb), and LY2940680 (Eli Lilly) (120). Currently, the only target for Phase I and II hedgehog inhibitors is SMO, highlighting the need for alternate Hh pathway targets to decrease the potential for resistance emerging through SMO-binding mutations.

The proposed mechanisms for the dozens of preclinical Hh inhibitor candidates are much more diverse. These compounds target a range of components in the Hh pathway including Shh, SMO, GLI1 and GLI2. However, there is no guarantee that any of these will successfully make it to clinic. It is therefore worthwhile to further explore currently FDA approved compounds that may provide novel target for Hh therapy.

1.6. Mebendazole

1.6.1. Anthelminthic Properties

Helminth infections occur in 1.5 billion people worldwide, over 20% of the world's population (121). To address the endemic, there has been continuous research into the development and characterization of anthelmintic therapy for the last 60 years. As a result of this research effort, the current generation of anthelminthic compounds is extremely safe and effective in humans.

Mebendazole (methyl N-[6-(benzoly)-1H-benzamidazol-2-yl] carbamate; MBZ) is a US Food and Drug Administration approved anthelminthic that has been used to treat parasitic worms since 1968. MBZ is one of six antiparasitic drugs of the benzimidazole class that also includes albendazole (ABZ), fenbendazole (FBZ), and thibendazole (TBZ). While all benzimidazoles are used in veterinary medicine, only ABZ, TBZ, and MBZ are approved for use in humans (122).

MBZ's mechanism of action against nematode infestation was first proposed in 1975. MBZ functions in parasites by binding to the colchicine-sensitive site in free β-tubulin, inhibiting it from being polymerized into microtubules (123). Intracellular transport processes that are dependent on the formation of cytoplasmic microtubules are also impaired in the parasite. The immediate result is impaired uptake of glucose by intestinal cells in larval and adult parasites. Without glucose uptake the parasite soon depletes its glycogen stores. This results in a series of downstream effects including the degenerative change of the mitochondria germinal layer and lysosome release which ultimately lead to an interruption of ATP production. Without any available energy the

parasite is immobilized and eventually dies. All benzimidazoles share the same proposed mechanism against nematode infections (124).

1.6.2. Safety

MBZ is often prescribed in humans due to its minimal side effects and broad spectrum anthelmintic abilities. It is effective against roundworm, whipworm, threadworm, tapeworm and hookworm. Complete elimination of the parasite often can be accomplished with a single 500 mg dose, however a follow up dosage two weeks later is typically recommended. Due to its remarkable safety and tolerability MBZ remains among the most widely used drugs in infected adults, including pregnant women and children. The difference in MBZs effect between species is due to a difference in stability. The rate of dissociation of MBZ from nematode tubulin is an order of magnitude lower than from human tubulin (125).

Mebendazole has a long track record of safety, having been used against parasitic infection for over 40 years. There are multiple documented cases of MBZ serving as long term chemotherapy for echinococcosis (hydatid disease) with no adverse side effects even after more than 13 years of daily therapy (48 mg/kg/day) (126). Doses as high as 200 mg/kg/day have been safely and effectively administered for up to 48 weeks for the treatment of internal hydatid cysts (127, 128). Unlike many therapeutic agents, MBZ has also been proven to accumulate to therapeutically relevant doses in the cerebrospinal fluid when treating helminth infection in the central nervous system, justifying possible MBZ therapy for diseases that affect the brain (127). The only significant side effect of these high, chronic doses is bone marrow suppression that has only been observed in fewer than 5% of patients. Case reports suggest that this adverse effect is associated with

increased therapeutic effect, and is therefore probably caused by higher blood levels of MBZ in these patients. In supportive clinical settings, this untoward effect could be addressed easily by close monitoring of the patient.

A major issue with MBZ treatment is its poor absorption. MBZ's limited solubility in water and organic solvents exacerbate this problem as it is commonly delivered orally. At low does in healthy human volunteers, MBZ absorption ranges from 5-22%. As dosage increases, the rate of absorption lowers to 1-2% (129). While systemic absorption is low, serum levels of MBZ peak one to three hours after intake, at reported levels that range from 0.3- 1.7 μM (127, 130). Studies have shown improved bioavailability by up to 5-8 fold when taken with a meal rich in fatty foods (131).

1.6.3. Anti-Cancer Effects

1.6.3.1. Preclinical Data

The Riggins Laboratory at Johns Hopkins first discovered that experimental brain tumors were sensitive to benzimidazoles when their mice were no longer receptive to xenograft engraftment after veterinary fenbendazole treatment, which was initiated in response to a pinworm infestation of their mouse colony. Follow up studies confirmed that fenbendazole, and also several other benzimidazoles exhibited the ability to inhibit cancer growth *in vitro*. ABZ and MBZ showed the greatest potency (132). The efficacy of ABZ and MBZ was evaluated against several models of glioblastoma multiforme (GBM) *in vivo*, including mouse GL261 and human 060919. Of all the benzimidazoles tested, MBZ consistently showed the greatest therapeutic response. MBZ is able to

successfully cross the blood brain barrier and significantly extend survival both as a monotherapy and in combination with temozolomide, a standard therapy for GBM.

MBZ antitumor effects were first published in 2002, regarding its efficacy against several lung cancer models both *in vitro* and *in vivo* (133). The MBZ treatment of non small cell lung cancer cells caused mitotic arrest followed by apoptotic cell death, with caspase activation and cytochrome c release (134). It was also noted that MBZ induced abnormal spindle formation. MBZ was shown effective against adrenocortical carcinoma both *in vitro* and *in vivo*, while also successfully blocking an invasion assay of H295R cells (135).

In 2008, the Orlow group screened 2,000 compounds in search of a novel therapy that would show efficacy against melanoma, but would be nontoxic to melanocytes. Only ten compounds out of the entire library satisfied these criteria. Of the ten hits, surprisingly four were of the same benzimidazole class (MBZ, ABZ, FBZ, and oxybendazole) (136). Mebendazole exhibited the greatest degree of potency among the benzimidazoles. In multiple chemoresistant melanoma cell lines, MBZ reduced proliferation, and induced caspase cascade activation, and disrupted microtubule polymerization as seen in previous cancers. A follow up study confirmed the ability of MBZ to inhibit growth of melanomas *in vivo* as effectively as temozolomide (137). Both studies proposed that the growth suppression seen by MBZ treatment functions in part by inhibition B-cell lymphoma 2 (BCL-2) by phosphorylation and proteasomal degradation of X-linked inhibitor of apoptosis (XIAP).

MBZ was also identified by a second screen for compounds with efficacy against colon cancer in 2013. 68 compounds exhibited cytotoxicity including members of the

benzimidazole class: MBZ, ABZ, FBZ, and oxybendazole (138). ABZ and MBZ had their efficacy analyzed against the NCI 60 cell line panel and surprisingly showed only modest correlation between the two compounds (Pearson's correlation coefficient of 0.64). The investigators explored the difference in efficacy between the two FDA approved benzimidazoles by testing their binding affinities at 10 μM in a high throughput binding assay. MBZ had interactions with several protein kinases which ABZ did not, including BCR-ABL, BRAF, PDGFRA, MEK1, KIT, JNK1, and more. An unrelated study used a novel rapid computational proteochemometric method that predicted and confirmed that MBZ was able to bind directly to VEGFR2 kinase and inhibit angiogenesis in human umbilical vein endothelial cells (HUVEC) cells (139). When testing the inhibitory effect of MBZ in various colon cancer lines this group found that MBZ shows greater growth suppression against cancer lines over immortalized fibroblasts (138).

The anticancer effect of MBZ defies a simple explanation. MBZ and related compounds have been reported to cause growth arrest and induce apoptosis in cultured cancer cells at doses that have little effect on non-cancer immortalized cells (133, 134, 136, 138, 140). The initial MBZ paper also noted this differential effect as both lung cancer lines A549 and H460 were substantially inhibited at 10 μM of MBZ, but the same dose had no effect on the proliferation of either HUVEC or WI-38 (lung fibroblasts) (133).

Since the initial report documenting the efficacy of MBZ in human cancer, there have been several proposed mechanisms. Most studies assumed the anticancer effect of MBZ was a consequence of microtubule inhibition that can lead to impaired structural

cellular integrity that affects cell division, cellular transport and migration (123). It is unclear why nonspecific antiproliferative effects of tubulin inhibition would preferentially target tumor cells over the cells in normal renewing tissues. Alternative mechanisms of MBZ have also been proposed including VEGF and HIF-1α inhibition and BCL-2 inactivation (135, 139). In lung cancers, MBZ was able to arrest cells at the G_2-M phase before the onset of apoptosis from cytochrome c release (133). In addition, a reduction of angiogenesis was seen in MBZ treated lung tumors. The possibility of MBZ inhibiting of critical enzymes through its unique structure has been proposed as well (138, 139).

1.6.3.2. Case Reports

Patient case studies provide some of the most convincing data regarding the anticancer effects of MBZ. The first case report on MBZ in cancer was published in 2010. In this case, a patient with metastatic adrenocortical carcinoma was treated with MBZ as a monotherapy (141). After surgical resection of the tumor, systemic chemotherapeutic treatments of 5-fluorouracil, streptozotocin, bevacizumab, and mitotane did not stop disease progression. MBZ was considered as a potential therapy for the patient based on its successful inhibition of adrenocortical carcinoma growth in both *in vitro* and *in vivo* models. All other chemotherapeutic therapies were ceased and the patient began MBZ monotherapy at standard anthelmintic dosing of 100 mg, twice daily. For pain control, the patient also received palliative radiation to the right adrenal metastasis. After two months of MBZ monotherapy the diameter of the hepatic metastases had decreased 17-42%. The metastases remained stable for 19 months of monotherapy without any adverse effects. The patient quality of life returned back to

baseline during treatment without symptoms of nausea or weight loss and had no abnormalities in his metabolic panel with a complete blood cell count. As is characteristic with most chemotherapeutic agents in adrenocortical carcinoma, response is generally short lived and subsequent disease progression occurred in the patient following 24 months of continuous MBZ monotherapy. The case documents the first successful application of long-term MBZ treatment against cancer progression without any adverse side effects.

A second case report of MBZ as a monotherapy against metastatic colon cancer was published as a follow up to the preclinical findings in 2013 (142). A 74 year old male presented with an advanced sigmoid colon cancer and multiple bilateral lung and paraaortic lymph node metastases. First line therapy involved palliative chemotherapy with capecitabine, oxaliplatin, and bevacizumab. However, due to neuropathy induced by oxaliplatin, an alternative second line therapy with irinotecan was instated. Disease progression was observed in lungs and abdominal lymph nodes and presentation of new metastases on the liver. Without any standard therapeutic options remaining, the patient consented to MBZ monotherapy based on previous preclinical data supporting efficacy against colon cancer. The patient followed the same dosage pattern of the first case report of oral delivery of 100 mg twice a day. Treatment continued for six weeks with no adverse effects. CT evaluation showed significant liver metastases regression and near complete remission of lung and lymph node metastases. Elevated liver enzymes AST and ALT caused a temporary stop in MBZ then resumed treatment at half dose. Liver enzymes returned to normal and follow up CT scans confirmed stable remission with no

adverse side effects reported by the patient. Until CT scans indicate disease progression the patient is on strategic treatment interruption.

1.7. Specific aims and hypothesis of the dissertation

A diverse range of cancers that are characterized by activated Hh signaling are pre-clinically responsive to MBZ and structurally related benzimidazoles. Recently, Hh signaling has been shown to be active in many gliomas (143, 144), while Hh ligands or markers of downstream pathway activity have been detected in melanomas, lung cancers, ovarian cancers, adrenocortical cancers and colorectal cancers (5, 6, 77-80) , which are all responsive to MBZ (133-136, 138, 141, 145). Notably, unbiased screens for novel Hh inhibitors have previously identified drugs that interact with microtubules, including vinblastine, vincristine, and paclitaxel (106). These drugs potently inhibit mitosis and are therefore highly toxic. The specific effects of these compounds on components of the Hh pathway have not been reported.

The potential role of the human PTCH1 homologs in the canonical and noncanonical Hh pathways is unclear. I have two related hypotheses. First, I hypothesize that MBZ exerts its anticancer effects in whole or in part via inhibition of canonical Hh signaling. Second, I hypothesize that PTCH53 controls canonical and noncanonical Hh pathways and thereby contributes to p53-dependent inhibition of tumorigenesis.

Aim 1: Evaluate MBZ's ability to inhibit Hh signaling in vitro. Evaluate the ability of benzimidazoles as a class to effect Hh signaling. Test if MBZ is capable of inhibiting Hh-dependent cell proliferation and survival. Check for selective growth inhibition based on a cell's Hh dependency.

Aim 2: Evaluate MBZ's ability to inhibit Hh signaling in vivo.. Test if MBZ can inhibit the growth of experimental brain tumors in mice.

Aim 3: Determine the molecular target of MBZ anticancer activity. Restore different Hh components to determine the point of Hh interference by MBZ. Evaluate MBZ's effect on SMO translocation, ciliogenesis, and tubulin polymerization.

Aim 4: Compare MBZ to vismodegib Test MBZ's effect against vismodegib resistant models and the effect of combination of both compounds on Hh signaling.

Aim 5: Explore the effect of PTCH53 expression on canonical Hh signaling and on induction of interferon response genes. Test the effect of PTCH53 on the activation of GLI by SMO, and test the effect of PTCH53 on the induction of the interferon response genes

Chapter 2: Materials and Methods

2.1. Cell lines and cell cultures

Cultures of 293T and hTERT-RPE1 cells and *Smo-/-* mouse embryo fibroblasts (MEFs) were maintained in DMEM (Life Technologies) supplemented with 10% fetal bovine serum (FBS; Hyclone) and penicillin/streptomycin. DAOY and C3H10T1/2 mouse fibroblast cells were grown in Eagle's MEM (Life Technologies) supplemented with 10% FBS and penicillin/streptomycin. NIH3T3 cells were grown in DMEM supplemented with 10% calf serum. Shh Light II cells (93) were grown in DMEM with 10% calf serum and 0.4mg/ml geneticin and 0.15 mg/ml zeocin, both purchased from Life Technologies. HCT116 and RKO colorectal cancer cells and their isogenic derivatives (146) were cultured in McCoys 5A supplemented with 10% FBS. All cell lines were obtained from ATCC and validated by the supplier, except for *Smo-/-* mouse embryo fibroblasts which were a gift from James Kim.

2.2. Orthotopic tumors

Syngeneic GL261 glioma tumors were grown intracranially in 4-6 week old female *nu/nu* athymic mice (NCI-Fredrick) and treated with MBZ as previously described (132). Each brain was snap frozen after extraction and stored in liquid nitrogen until further analysis. Orthotopic medulloblastoma xenografts were generated in female athymic mice, 5-6 weeks of age (NCI). DAOY cells expressing luciferase were used for brain tumor implantation. For the implantation procedure, mice were first anesthetized. With a stereotactic frame, 100,000 DAOY cells were injected through a burr hole drilled

1 mm lateral to the right of the sagittal suture and 1 mm posterior to the lambda, at a depth of 2.5 mm below the dura at a rate of 1 µl/minute. Treatment was initiated at 5 days post implantation, when treated mice received a 25 mg/kg daily dose of MBZ, delivered with 50% (v/v) sesame oil and PBS, by gavage. Mice were euthanized when they showed signs of increased intracranial pressure. All animal protocols and procedures were performed under an approved protocol and in accordance with the Johns Hopkins Animal Care and Use Committee guidelines. For RNA preparation, each brain was thawed on ice before removing the right anterior cerebral cortex and the contralateral brain section. Each tissue sample was suspended in 1 mL of TRIzol (Life Technologies) per 0.1 g of material, and the RNA fraction was purified according to the manufacturer's recommendations.

2.3. Plasmids and cell transfections

ShhN-conditioned media was generated by transfection of pcDNA3 ShhN (provided by Pao Tien Chuang) into 293T cells. Control media was obtained from mock-transfected 293T cells. For localization of SMO, hTERT RPE-1 cells grown in chamber slides (Nunc) were transfected with pcDNA3 Smo-FLAG (provided by Chen Ming Fan). GLI1 reporter assays were conducted by cotransfecting the firefly luciferase reporter pBV Luc 8xGli (provided by Craig Peacock) and TK-renilla luciferase reporter pGL4 74 (Promega). Overexpression of Hh components was achieved by transient transfection of pRK-SmoM2 (147), pCMV5 hGLI1 FLAG (provided by Peter Zaphiropoulos), and pCS2-MT hGLI2 FL (Addgene plasmid 17648) (148). Mutant-*Smo* expression constructs were provided by James Kim. PTCH53 Hh suppression was analyzed by transient transfection of pCDNA3.1-PTCH53 (provided by Jon Chung), pCDNA3.1-PTCHD1-

Myc (provided by John Vincent) (149), pCI-PTCH1-FLAG (provided by Takashi Shimokawa) (150). All transfections were performed with FuGENE HD (Promega).

2.4. GLI-reporter assays and drug treatment

Subconfluent Shh Light II cells were routinely incubated in low serum conditions (0.25% fetal bovine serum, 5 mm HEPES), to optimize Hh responsiveness, during a 48 h period of drug treatment. For ShhN ligand stimulation, cells were incubated with ShhN-conditioned media or control media, diluted 1:5, during the treatment period. Final DMSO concentration in all cultures was 1%. For experiments involving overexpression of Hh pathway components, cells were transfected 24 h prior to low serum and drug treatment. Cell lysates were analyzed using the Dual Luciferase Assay Reporter System (Promega). GLI-dependent luciferase was measured on a Victor3 V 1420 Multilabel Counter (Perkin Elmer) and standardized against *renilla* luciferase activity. The IC_{50} was calculated by Prism 5 software package (GraphPad).

For the assessment of Gli-luc activity relative to *PTCH53* overexpression, *Smo-/-* mouse embryo fibroblasts were transfected with 200 ng Gli-luciferase reporter plasmid, 200 ng pGL4.74,150 ng SMO plasmid and varying mass ratios of PTCH1, PTCHD1, PTCH53 expression plasmids. Each well was split into three wells of a 24 well plate 8h after transfection, After 24 h, media was replaced with DMEM containing reduced serum (0.5% FBS). Lysates were collected for analysis 72 h after transfection. All experiments were performed in triplicate with at least 3 independent experiments.

2.5. Cell proliferation, viability and survival assays

BrdU incorporation during DNA synthesis was measured using the Cell Proliferation ELISA kit (Roche). Cell viability was measured with the Cell Titer-Blue Cell Viability Assay kit (Promega). Colorimetric signals were measured on a SpectraMax M5 (Molecular Devices). For each assay, the IC_{50} was calculated with the Prism 5 software package (GraphPad). For assessment of clonogenic survival, cells were drug-treated under low serum conditions in 12 well plates. After 48 h, cells were harvested in trypsin-EDTA (Life Technologies), diluted 1:4000 in standard growth media and seeded in 10 cm plates, in triplicate. After 10 days of growth, plates were stained with 0.2% crystal violet in 50% MeOH and destained in water. Colonies containing more than 50 cells were scored.

2.6. Immunoblots and immunofluorescence

Proteins were separated on Bis-Tris gels (Life Technologies) and transferred onto Immobilion-P nylon membranes (Millipore). Following overnight incubation with primary antibodies under standard conditions, blots were developed with HRP-conjugated secondary antibodies and visualized by chemiluminescence (Amersham). Band intensities were quantified by Image Lab software and standardized to the intensity of the loading controls anti-α-tubulin or anti-β-actin. To assess tubulin polymerization, polymerized and unpolymerized tubulin fractions were separated on the basis of solubility as reported previously (151).

For analysis of primary cilia by immunofluorescence, cells were grown on poly-D-lysine (Sigma) coated chamber slides (Nunc) and fixed in 0.4% paraformaldehye at 37°C for 5 min, permeabilized in 0.5% Triton X-100 at 37°C for 2 min, washed in PBS, then sequentially incubated in 4% paraformaldehyde, 37°C for 5 min, and methanol, -

20°C for 5 min, as previously described (152). Nonspecific proteins were blocked with 2% bovine serum albumin in PBS for 30 min at RT. Slides were incubated with primary antibody in blocking buffer overnight at 4°C, then washed with PBS and incubated with either biotinylated (Santa Cruz Biotechnology) o/r Alexa Fluor 594-conjugated (Life Technologies) secondary antibodies in blocking buffer for 20 min at room temperature. Cells were washed with PBS before adding an Alexa Fluor 488-streptavidin conjugate (Life Technologies). Nuclei were counterstained with 4',6-diamidino-2-phenylindole (DAPI; Life Technologies). Stained cells were visualized with an AxioImager Z1 (Carl Zeiss) and images were captured with Axiovision Rel 4.6 software.

The following primary antibodies were used: anti-GLI1 (C68H3; Cell Signaling), anti-cleaved caspase 3 (D175; Cell Signaling), anti-α-tubulin (TU-02; Santa Cruz), HRP-conjugated anti-β-actin (Santa Cruz), anti-acetylated α-tubulin (6-11 B-1; Sigma), anti-FLAG (anti-DYKDDDDK; Cell Signaling), anti-MX2 (N-17; Santa Cruz).

2.7. Quantitative real time RT-PCR

RNA was isolated and purified with the TRIzol reagent (Life Technologies), treated with DNase I (Thermo Scientific) and assayed by spectrophotometry. cDNA was synthesized with the Maxima First Strand cDNA synthesis kit (Thermo Scientific). Quantitative, real time reverse-transcription PCR (qRT-PCR) was performed using both Maxima Probe and Maxima SYBR Green qPCR Master Mixes (Thermo Scientific) with standard cycling conditions on a 7900HT Fast Real-Time PCR system (Applied Biosystems). Prime Time qPCR probes and primers were used to assay the mouse genes: *Ptch1*: probe (5'-ATTCGGACCCTGCAAGCATCAGT-3'), forward primer (5'-

TGTTTGCTCCCGTTCTGG-3'), reverse primer (5'-AACCAGTCCATTGAGAACCC-3'); *Gli1*: probe (5'-CTGGGACCCTGACATAAAGTTGGCT-3'); forward primer (5'-CTTTCTGGTCTGCCCTTTTG-3'); reverse primer (5'-TCTTTGTTAATTTGACTGAACTCCG-3'); *Rpl19*: probe (5'-CTTCTCAGGAGATACCGGGAATCCAAG-3'); forward primer (5'-AGAAGGTGACCTGGATGAGAA-3'); reverse primer (5'-TGATACATATGGCGGTCAATCT-3'). Human transcripts were analyzed with SYBR green. *GLI1*: forward primer (5'-CCACGGGGAGCGGAAGGAG-3'); reverse primer (5'-ACTGGCATTGCTGAAGGCTTTACTG-3'). *PTCH1*: forward primer (5'-CCACAGAAGCGCTCCTACA-3'); reverse primer (5'-CTGTAATTTCGCCCCTTCC-3'). *GAPDH*: forward primer (5'-CGGAGTCAACGGATTTGGTCGTAT-3'); reverse primer (5'-AGCCTTCTCCATGGTGGTGAAGAC-3'). *PTCH53*: forward primer (5'-AAGCCAGCTCTATTCGGACTTAC-3'); reverse primer (5'-ACTTGACCCGCTGATCTTTG-3'). *CDKN1A*: forward primer (5'-ACAGCAGAGGAAGACCATGTG-3'); reverse primer (5'-GGGCTTCCTCTTGGAGAAGAT-3'). *PTCH1*: forward primer (5'-CCACAGAAGCGCTCCTACA-3'); reverse primer (5'-CTGTAATTTCGCCCCTTCC-3'). *BST2*: forward primer (5'-CACACTGTGATGGCCCTAATG-3'); reverse primer (5'-GTCCGCGATTCTCACGCTT-3'). *IFI27*: forward primer (5'-TGCTCTCACCTCATCAGCAGT-3'); reverse primer (5'-CACAACTCCTCCAATCACAACT-3'). *IFI44L*: forward primer (5'-AGCCGTCAGGGATGTACTATAAC-3'); reverse primer (5'-AGGGAATCATTTGGCTCTGTAGA-3'). *IFI6*: forward primer (5'-

GTCTGCGATCCTGAATGGG-3'); reverse primer (5'-TCACTATCGAGATACTTGTGGGT-3'). *IFIH1*: forward primer (5'-TCGAATGGGTATTCCACAGACG-3'); reverse primer (5'-GTGGCGACTGTCCTCTGAA-3'). *IFIT1*: forward primer (5'-TTGATGACGATGAAATGCCTGA-3'); reverse primer (5'-CAGGTCACCAGACTCCTCAC-3'). *IFITM1*: forward primer (5'-TGATCAACATCCACAGCGAGAC-3'); reverse primer (5'-TCCTGTCCCTAGACTTCACGGA-3'). *ISG15*: forward primer (5'-CGCAGATCACCCAGAAGATCG-3'); reverse primer (5'-TTCGTCGCATTTGTCCACCA-3'). *MX2*: forward primer (5'-CAGAGGCAGCGGAATCGTAA-3'); reverse primer (5'-TGAAGCTCTAGCTCGGTGTTC-3'). *OAS1*: forward primer (5'-TGTCCAAGGTGGTAAAGGGTG-3'); reverse primer (5'-CCGGCGATTTAACTGATCCTG-3'). *OAS2*: forward primer (5'-CTCAGAAGCTGGGTTGGTTTAT-3'); reverse primer (5'-ACCATCTCGTCGATCAGTGTC-3'). *OAS3*: forward primer (5'-GAAGGAGTTCGTAGAGAAGGCG-3'); reverse primer (5'-CCCTTGACAGTTTTCAGCACC-3'). *OASL*: forward primer (5'-CTGATGCAGGAACTGTATAGCAC-3'); reverse primer (5'-CACAGCGTCTAGCACCTCTT-3'). *SAMHD1*: forward primer (5'-CTGGAACTCCATCCCGACTAC-3'); reverse primer (5'-AGTAATGCGCCTGTGATTTCAT-3'). *USP18*: forward primer (5'-CCTGAGGCAAATCTGTCAGTC-3'); reverse primer (5'-

CGAACACCTGAATCAAGGAGTTA-3'). All results were analyzed using SDS RQ Manager (Applied Biosystems).

2.8. Interferon and interferon stimulating DNA

All cells treated with human IFN-α1 (Cell Signaling) were treated at 100ng/mL in low serum conditions. Cells were transiently transfected with interferon stimulating DNA (ISD) and ISD Control (InvivoGen) at 1 μg/mL with FugeneHD for 24 h before changing to low serum for 48 h.

2.9. Statistics

Two-tailed t-tests were used to assess significance. *, $p<0.05$ **, $p<0.02$ ***, $p<0.005$. Error bars indicate standard error of the mean unless otherwise indicated. For survival curve comparison, the Prism 5 software package (GraphPad) was used to calculate significance with both the Mantel-Cox test and Gehan-Breslow-Wilcoxon test.

Chapter 3: Results

3.1. Mebendazole inhibits Hh signaling

To directly assess the effect of MBZ on canonical Hh signaling, we incubated the drug with murine Shh-Light II cells, which have stably incorporated a GLI-activated firefly luciferase (Gli-luc) reporter construct (93). Under low serum conditions that are optimal for Hh activation, addition of the amino-terminal signaling domain of the secreted Sonic Hedgehog ligand (ShhN) induced robust reporter activity that could be inhibited by MBZ in the micromolar dose range **(Fig. 3.1.A)**. A similar degree of inhibition was observed in mouse C3H10T1/2 fibroblast cells transiently transfected with the Gli-luc reporter **(Fig. 3.1.B)**. MBZ was a considerably more potent inhibitor of Hh pathway activation than structurally related antihelminthic drugs **(Fig. 3.2)**, which in prior studies were less effective than MBZ at inhibiting the growth of GL261 gliomas (132). The GL261 mouse tumor harbors a mutation in *Pten* (153); in humans, mutation of *PTEN* defines a category of gliomas that are strongly associated with elevated Hh activity (144). We assessed endogenous *Gli1* transcript levels in MBZ-treated and control GL261 tumors. *Gli1* expression was significantly elevated in untreated tumors compared with non-affected tissue from the contralateral side of the brain **(Fig. 3.3.A)**, suggesting a role for Hh signaling in the growth of these tumors. *Gli1* expression in tumor tissues was decreased by MBZ treatment **(Fig. 3.3.B)**. To extend our analysis to human cells, we tested the effects of MBZ on Hh-mediated gene expression in the immortalized human retinal pigment epithelial cell line hTERT-RPE1. Unlike the majority of human cancer cell lines, this non-cancer cell line is responsive to ShhN **(Fig. 3.4)**. A concentration of

0.1 μM MBZ was sufficient to reduce ShhN-induced expression of endogenous *GLI1* and *PTCH1* to basal levels **(Fig. 3.4)**. Further Hh pathway inhibition was observed at higher MBZ concentrations.

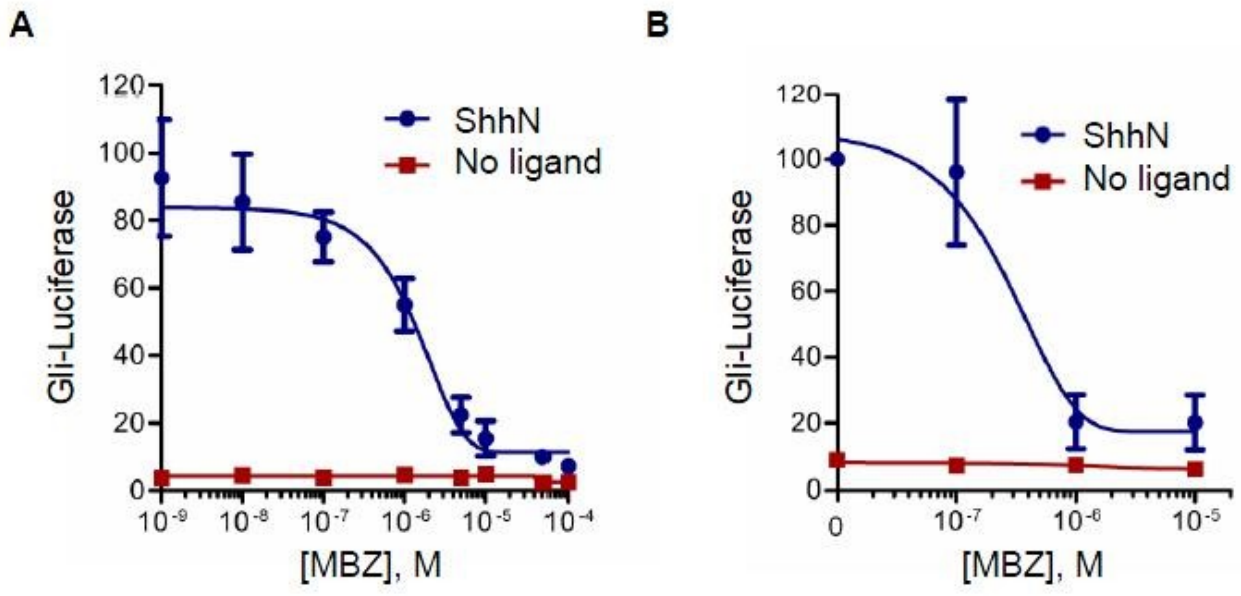

Figure 3.1. MBZ inhibits Gli1 in luciferase reporter system

(A) Shh-Light II cells maintained in low serum conditions were incubated in ShhN-conditioned medium or control medium, in the presence of MBZ at the indicated concentrations. The activity of the stably integrated Gli-luc reporter was measured after 48 h of treatment. **(B)** C3H10T1/2 mouse fibroblasts were co-transfected with the Gli-luc and *renilla* luciferase reporters. After 24 h, MBZ was added for an additional 48 h in low serum media prior to cell lysis and measurement of luciferase activity.

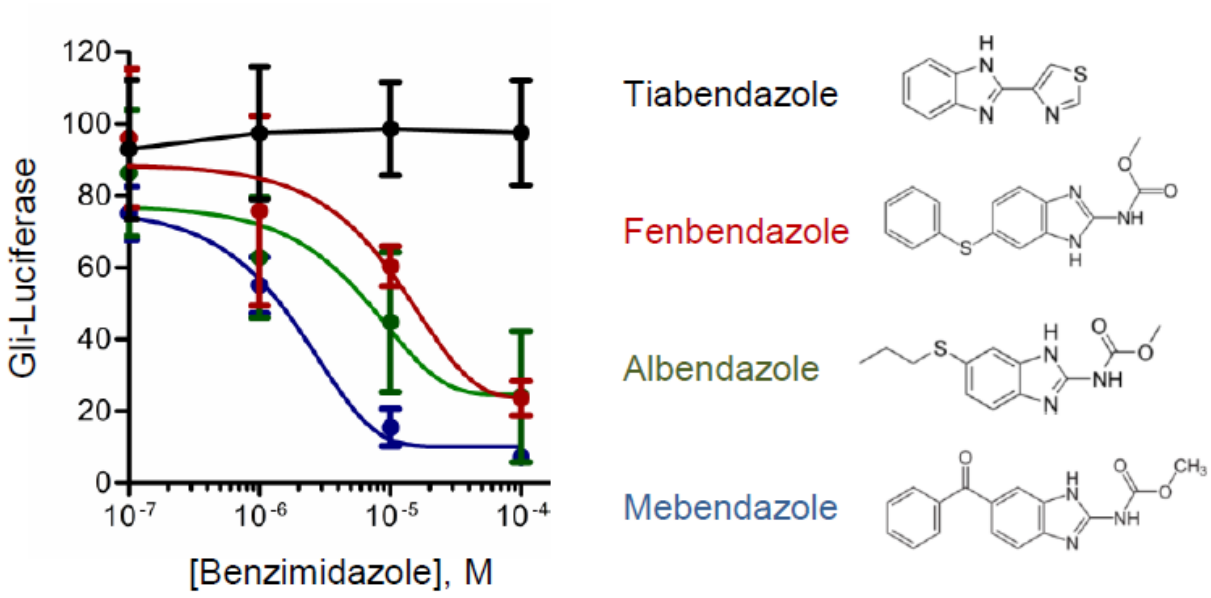

Figure 3.2. Hh inhibition by benzimidazoles

The effect of MBZ on Gli-luc reporter activity in Shh-Light2 cells was compared with that of the structurally related benzamidizoles albendazole, fenbendazole, and tiabendazole. Treatment times and conditions were as in **Fig 3.1A**.

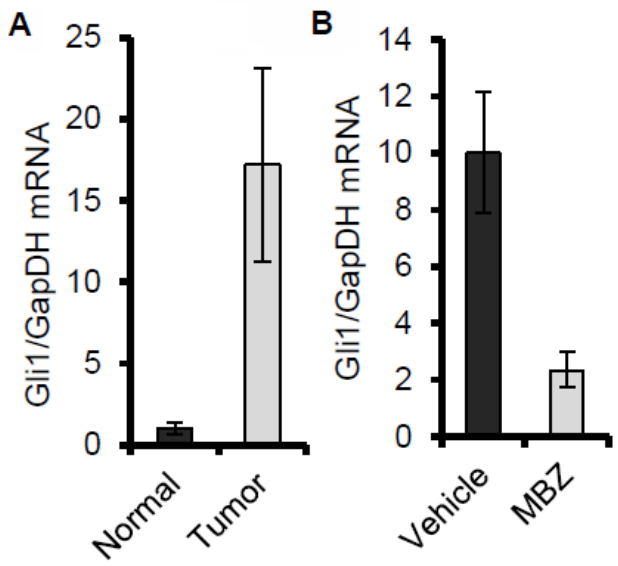

Figure 3.3. MBZ inhibits Hh signaling in GL261 *in vivo*

(A) Endogenous levels of *Gli1* transcripts in syngeneic, GL261 gliomas and in normal brain tissue from the contralateral region were measured by qRT-PCR. **(B)** *Gli1* expression was measured by qRT-PCR in untreated and MBZ-treated GL261 tumors. Each measurement was standardized to a parallel measurement from a contralateral brain section that did not contain tumor tissue.

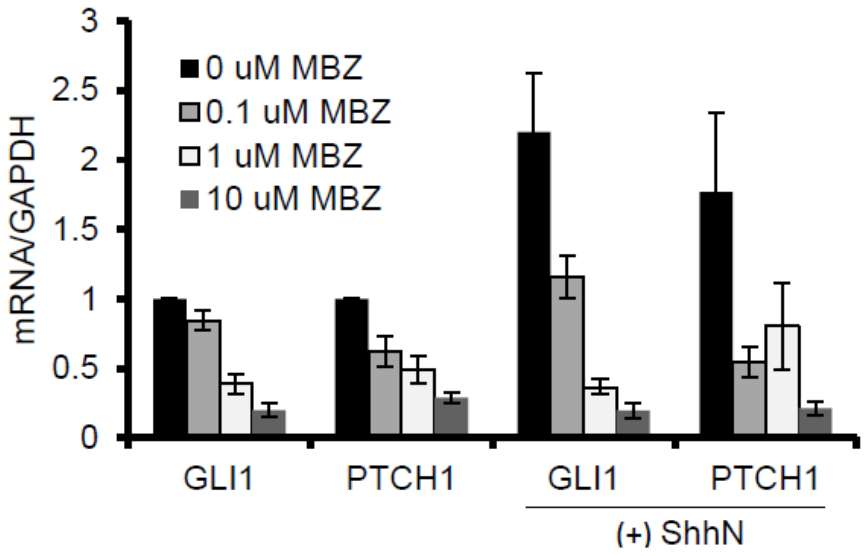

Figure 3.4. MBZ suppresses GLI1 and PTCH1 in hTERT-RPE1 cells *in vitro*

hTERT-RPE1 cells growing in low serum were treated with ShhN-conditioned or control medium for 48 h. MBZ was included during this treatment period at the concentrations indicated. Transcript levels were assessed by qRT-PCR.

3.2. Effect of mebendazole on Hh signaling, growth and survival of Hh dependent medulloblastoma cells

The effects of MBZ on Hh-dependent cell proliferation and survival were next assessed in the human medulloblastoma cell line DAOY. DAOY cells have a gene expression profile consistent with a type 2 (Hh-subtype) medulloblastoma and accordingly exhibit elevated Hh signaling (154). MBZ caused a reduction in *GLI1* expression, IC_{50}=516 ±81 nM (SEM); **(Fig. 3.5.B)** and could also inhibit the increased expression of *GLI1* and *PTCH1* observed after addition of ShhN ligand **(Fig. 3.5.A)**. At similar concentrations MBZ markedly inhibited DAOY cell proliferation **(Fig. 3.6.A)** and reduced clonogenic survival **(Fig. 3.6.B)**. The viability of DAOY cells was significantly impaired by MBZ at concentrations approaching 1 μM. In contrast, hTERT RPE-1 cells, which are Hh-responsive but not dependent on Hh signals for growth, were only modestly affected **(Fig. 3.7.A)**. The expression of GLI1 protein was similarly reduced in both cell types by increasing concentrations of MBZ, but only DAOY cells exhibited biochemical (**(Fig. 3.7.B)** and morphological **(Fig. 3.8)** evidence of apoptosis. When injected into the cerebella of nude mice to form orthotopic xenografts, DAOY cells were responsive to MBZ administered by daily gavage. MBZ treatment suppressed levels of *GLI1* transcripts in the DAOY-derived tumors **(Fig. 3.9.A)** and significantly extended survival (p=0.01; **Fig. 3.9.B)**. Notably, DAOY xenografts exhibit large cell morphology (154), which in naturally-evolving tumors is associated with poor outcomes (155).

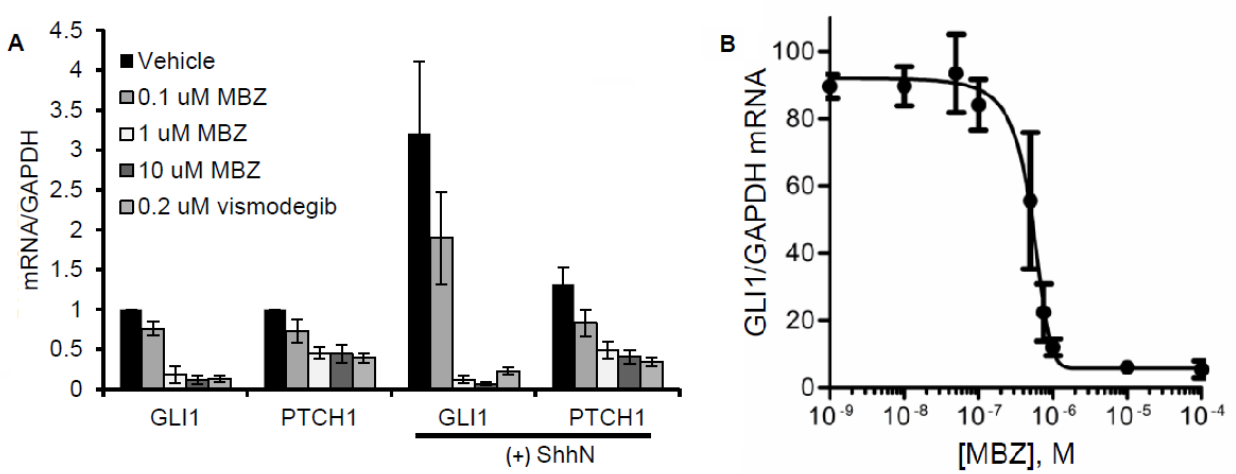

Figure 3.5. MBZ suppresses GLI1 and PTCH1 in DAOY cells *in vitro*

(A) Subconfluent DAOY cells were incubated under low serum conditions with ShhN-conditioned or control medium for 48 hrs and treated during this period with MBZ at varying concentrations. Transcript levels were assessed by qRT-PCR. **(B)** DAOY cells were grown for 48 hours in low serum conditions with a range of MBZ concentrations and *GLI1* expression was assayed by qRT-PCR.

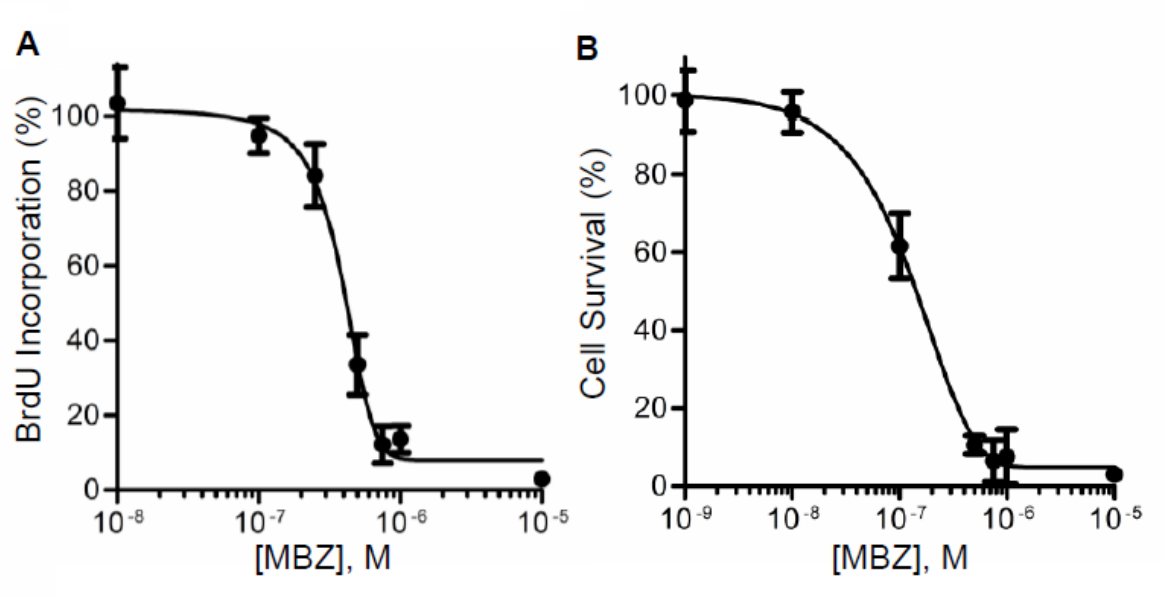

Figure 3.6. MBZ reduces proliferation and clonogenicity in DAOY cells

Subconfluent DAOY cells were incubated under low serum conditions for 48 hrs and treated during this period with MBZ at varying concentrations. **(A)** Cell proliferation was assessed by measuring the incorporation of BrdU over 2 h, following drug treatment. **(B)** Cell survival was quantified by a clonogenic assay after drug treatment.

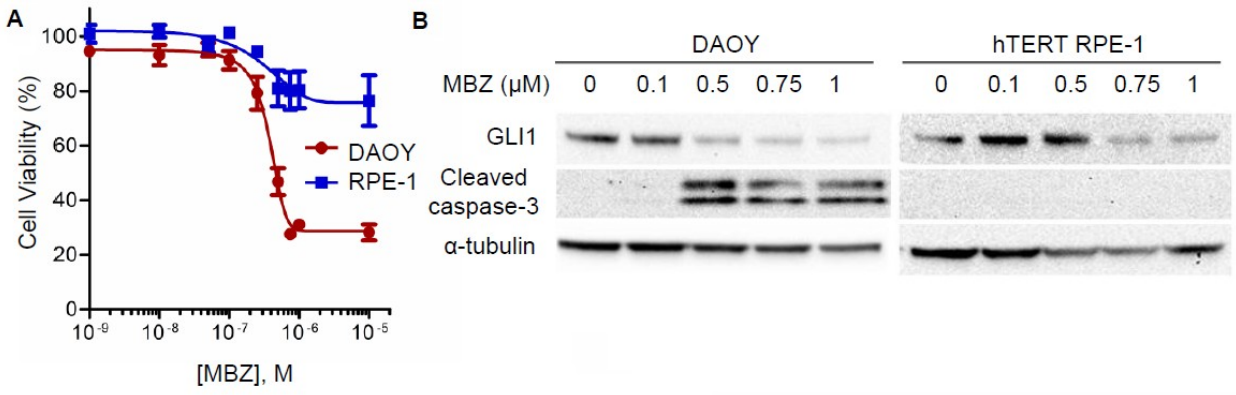

Figure 3.7. MBZ effect on cell viability of DAOY and hTERT-RPE1 cells

Subconfluent DAOY cells were incubated under low serum conditions for 48 hrs and treated during this period with MBZ at varying concentrations. **(A)** The effect of MBZ on cell viability was comparatively assessed by CellTiter-Blue in hTERT-RPE1 (blue) and DAOY (red). **(B)** The expression of GLI1 protein and cleavage of caspase-3 were assessed by immunoblot in DAOY and hTERT-RPE1 cells treated with MBZ for 12 h, under low serum conditions. α-tubulin was assessed as a loading control.

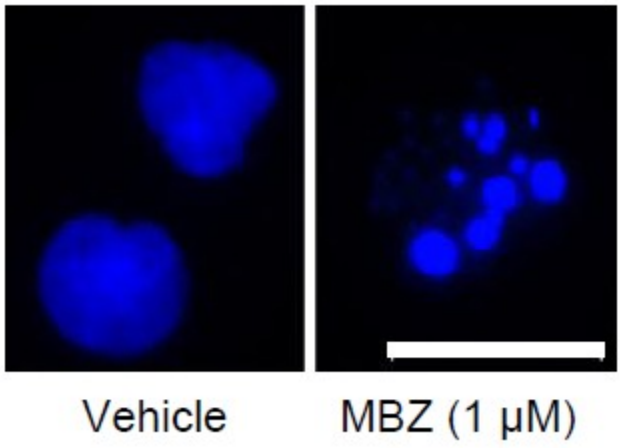

Figure 3.8. Apoptosis in DAOY cells

DAOY cells incubated under the same conditions as **Fig 3.6.** Representative nuclei from MBZ-treated DAOY cells and untreated controls, stained with Hoechst 33258. Scale bar, 20 µm.

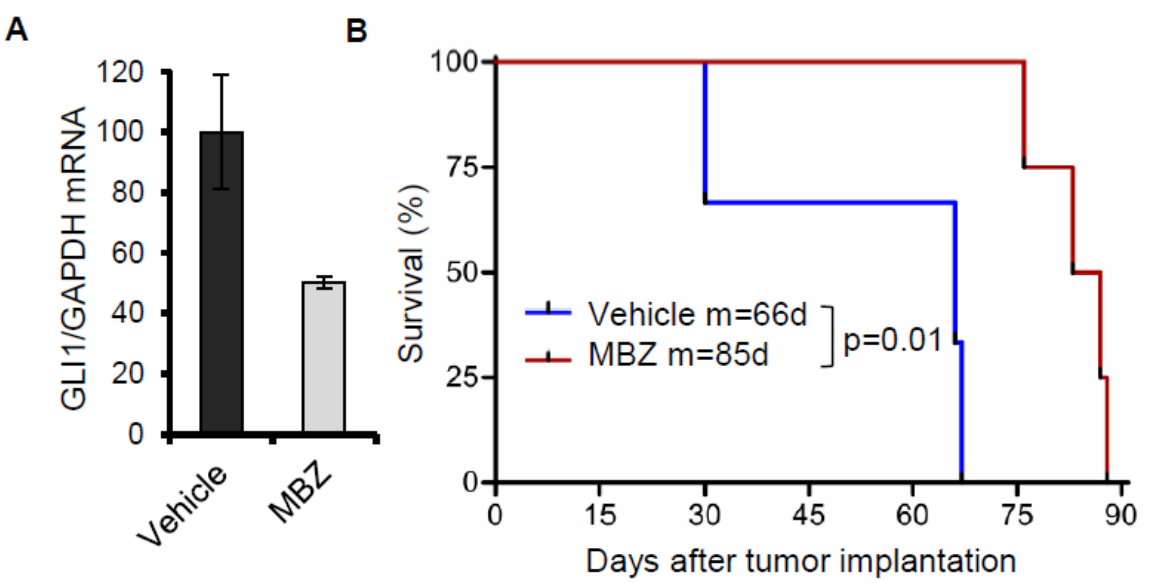

Figure 3.9. MBZ extends survival and inhibits GLI1 expression in DAOY cells grown as xenograft tumors *in vivo*

(A) DAOY cells were grown as orthotopic xenografts following injection into the cerebella of nude mice. After 5 d, mice were treated with 25 mg/kg MBZ (n=4) or mock-treated (n=3). One mouse from the mock treatment group did not develop symptoms of a growing brain tumor, and was euthanized after surviving for more than six months. This mouse was not found to have a brain tumor, and was therefore omitted from this analysis. Total RNA was harvested from representative tumors at the time of death and *GLI1* transcripts were quantified by qRT-PCR. **(B)** Survival of mice with DAOY-derived orthotopic tumors.

3.3. Mebendazole inhibits activation of SMO

We next tested the ability of MBZ to counteract Hh signaling induced by individual components of the pathway. NIH3T3 cells strongly activated the Gli-luc reporter in response to ShhN-conditioned medium; this upregulation of Hh activity was suppressed by MBZ and by vismodegib **(Fig. 3.10.A)**. Hh signaling could also be strongly stimulated in these cells by transient overexpression of the Ptch1-resistant SmoM2 mutant protein (147), and by GLI1 or GLI2 **(Fig. 3.10.B)**. The stimulatory effect of SmoM2 on Gli-luc activation could be suppressed by MBZ, whereas reporter activation by the downstream effectors GLI1 and GLI2 was resistant to MBZ **(Fig. 3.11)**.

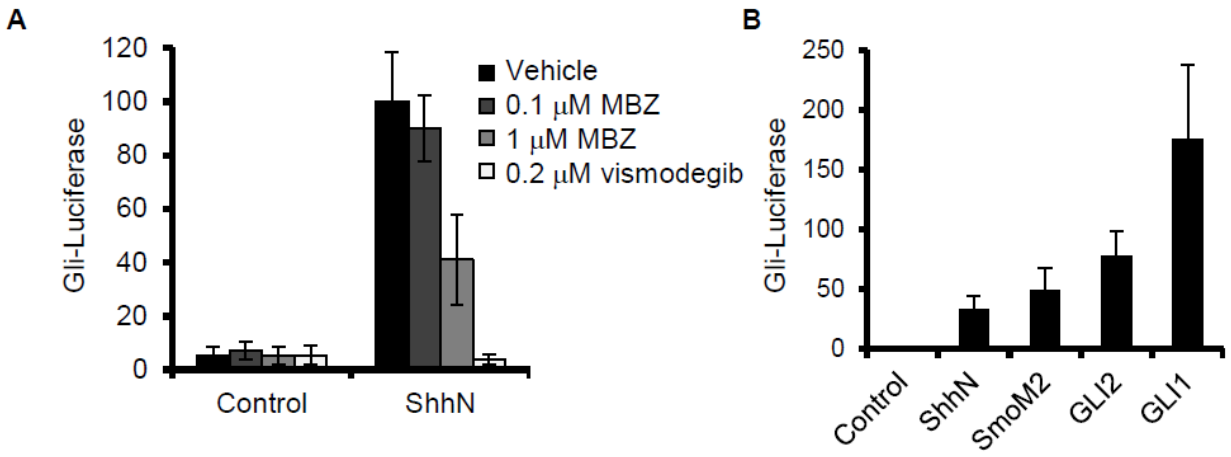

Figure 3.10. Relative Gli1 stimulation in 3T3 cells

(A) NIH3T3 fibroblasts co-transfected with Gli-luc and *renilla* reporter plasmids were maintained in low serum conditions for 48 h in the presence of ShhN-conditioned or control media. During this period, MBZ or vismodegib were added at the indicated concentrations. **(B)** A direct comparison of Gli-luc activation in NIH3T3 cells 48 h after treatment with ShhN ligand, or 72 h after cotransfection with plasmids that drive exogenous expression of the Ptch1-resistant Smo mutant SmoM2, GLI1 or GLI2 in low serum media.

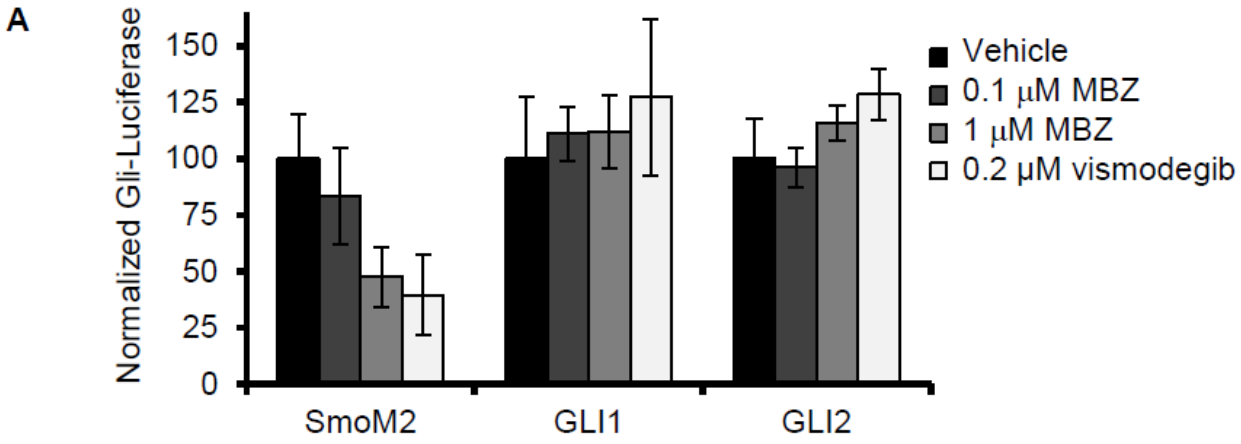

Figure 3.11. Gli1 signaling rescued from MBZ by restoration of Hh components

MBZ or vismodegib was added to SmoM2-, GLI1-, or GLI2-transfected NIH3T3 cells during 48 h of incubation in low serum conditions. The activation of a co-transfected Gli-luc reporter by each overexpressed gene, in the absence of drug treatment, was normalized to 100.

3.4. Mebendazole inhibits formation of primary cilia

To assess the effect of MBZ on upstream signaling by SMO, we examined the cellular localization of a Smo-FLAG fusion protein (156) by immunofluorescence. Under low serum conditions that favor primary cilium formation and robust SMO activation, Smo-FLAG was predominantly localized to the primary cilia **(Fig. 3.12)**. MBZ-treated cells exhibited a notable paucity of primary cilia. In non-ciliated cells Smo-FLAG was distributed throughout the cytoplasm **(Fig. 3.12)**. The suppressive effect of MBZ on ciliogenesis was quantified in larger cell populations **(Fig. 3.13.A** and **Fig. 3.13.B)**. The proportion of ciliated cells decreased in response to MBZ within a concentration range that also inhibited the polymerization of human β-tubulin *in vitro* **(Fig. 3.14.A and 3.14.B)**. We next tested whether allowing primary cilia to pre-form prior to MBZ addition could alter the effect of MBZ on pathway activity. Temporally separating serum starvation from MBZ administration partially restored *GLI1* expression **(Fig. 3.15.A)** and viability **(Fig. 3.15.B)** in MBZ-sensitive DAOY cells.

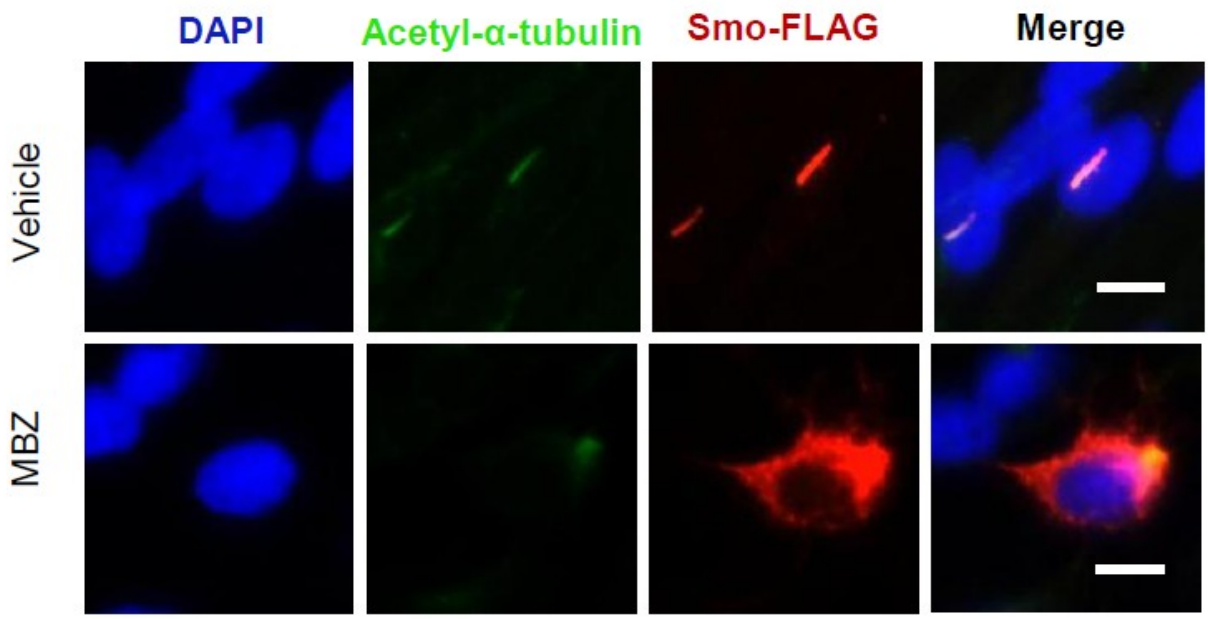

Figure 3.12. Visualizing Smo localization relative to primary cilia

A Smo-FLAG fusion protein was expressed in hTERT-RPE1 cells following transient transfection. After 48 h incubation in low serum and treatment with 1 uM MBZ or vehicle, cells were fixed, permeabilized and stained with antibodies directed against acetyl-α-tubulin (green) and FLAG (red). Nuclei were counterstained with DAPI. Scale bar, 10 μm.

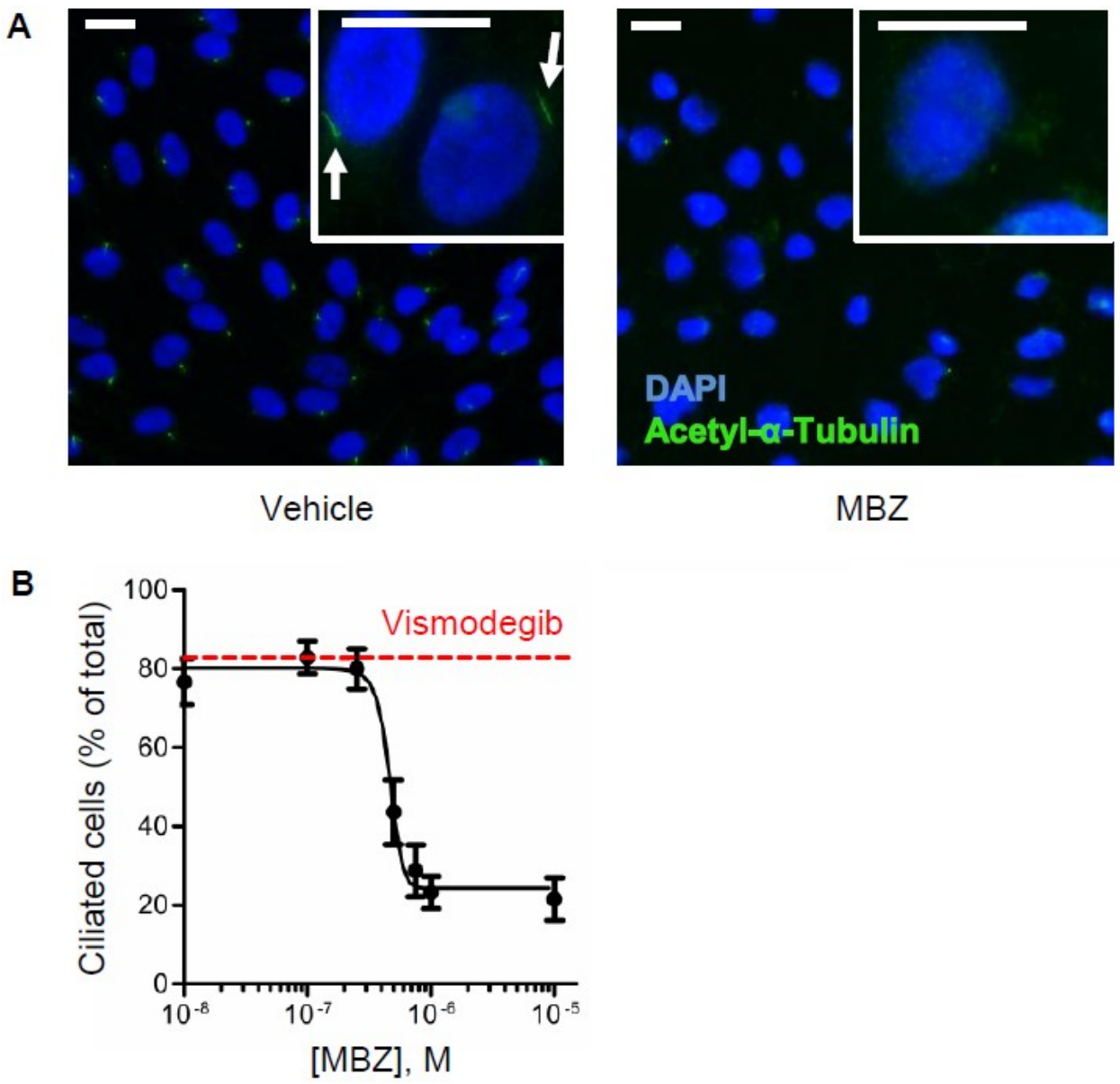

Figure 3.13. MBZ quantitatively inhibits ciliogenesis

(A) Cilia were numerically assessed by acetyl-α-tubulin staining in hTERT-RPE1 cells maintained in low serum conditions and treated with MBZ. Primary cilia (indicated by arrows) could be visualized on individual cells (inset). Scale bar, 20 µm. **(B)** The effects of MBZ or 0.2 µM vismodegib (red line) on the proportions of ciliated cells, expressed as a total of the cell population.

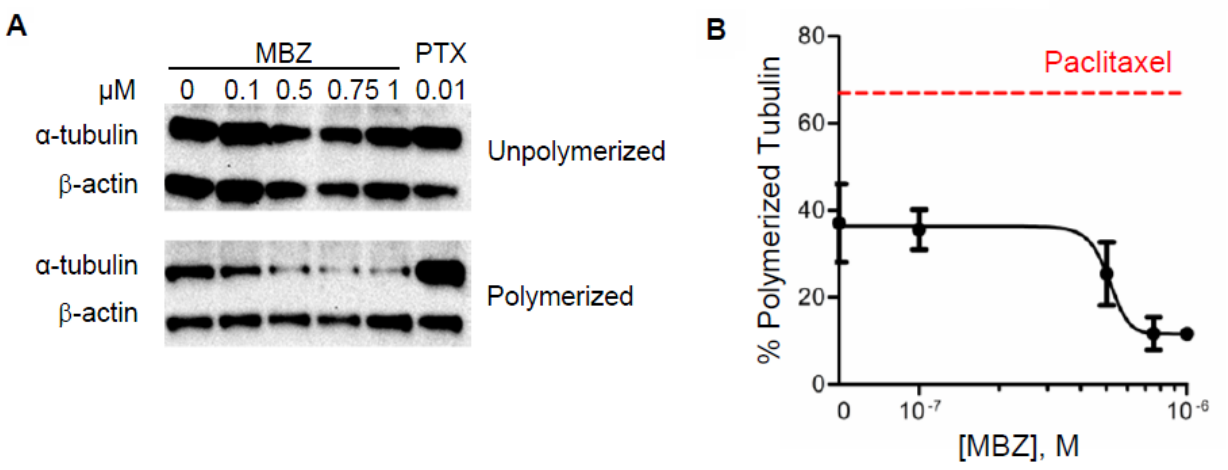

Figure 3.14 MBZ inhibits tubulin polymerization

hTERT-RPE1 cells were treated with MBZ at the indicated concentrations or with 10 nM paclitaxel (red line) for 48 h under low serum conditions. Polymerized and unpolymerized tubulin fractions were quantified by immunobloting, **(A)** normalized to the loading control β-actin, and expressed as the proportion of polymerized tubulin compared to the combined polymerized and unpolymerized tubulin **(B)**.

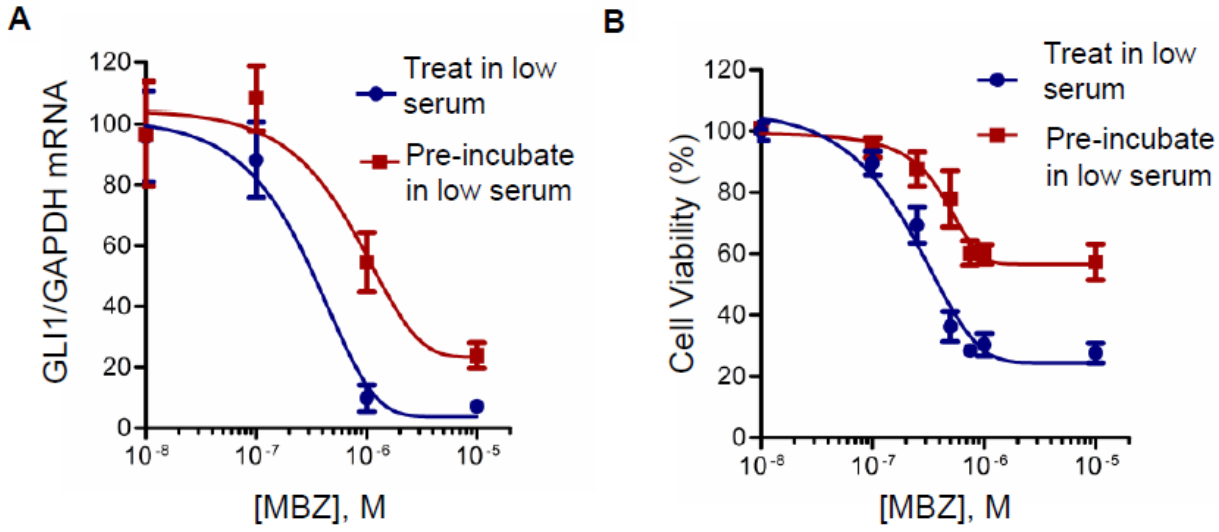

Figure 3.15. Serum starvation reduces MBZ effect on GLI1 and proliferation

(A) *GLI1* expression was assessed in DAOY cells that were incubated with MBZ for 48 h under the low serum conditions that allow formation of the primary cilium ("Treat in low serum"), or that were first maintained in low serum for 20 h prior to before adding MBZ for an additional 48 h ("Pre-incubate in low serum"). **(B)** Cell viability was assessed by CellTiter-Blue after the treatments described in **(A)**.

3.5. Additive effect of mebendazole and vismodegib against SMO-dependent, canonical Hh signaling

3.5.1. MBZ inhibits vismodegib resistance Smo

As MBZ exerts an indirect effect on SMO, we reasoned that MBZ might inhibit the activity of mutant SMO proteins that have been found to confer vismodegib resistance. To test this idea, we assayed the ability of MBZ to inhibit Gli-luc activation by wild type and vismodegib-resistant mutant Smo proteins exogenously expressed in *Smo*$^{-/-}$ mouse embryo fibroblasts. Gli-luc activity was induced by Shh ligand in the presence of either wild type *Smo* or the *Smo* D477G mutant. This mutation was originally found in a vismodegib-resistant allograft derived from a mouse medulloblastoma and corresponds to an equivalent mutation found in a patient with recurrent disease (103). Activation of Gli-luc by *Smo* D477G was completely resistant to inhibition by vismodegib **(Fig. 3.16.A)**. In contrast, both wild type and mutant Smo could be functionally suppressed by MBZ **(Fig. 3.16.B)**. Analysis of an expanded panel of all described vismodegib-resistant *Smo* mutants (104) confirmed that the inhibitory effects of MBZ were unaffected by the vismodegib-selected alterations in Smo **(Fig. 3.17)**.

3.5.2. Additive effect

When used in combination **(Fig. 3.18.A and Fig. 3.18.B)**, vismodegib and MBZ additively suppressed the Gli-luc signal **(Fig. 3.19)**, a result that is consistent with two independent modes of pathway inhibition.

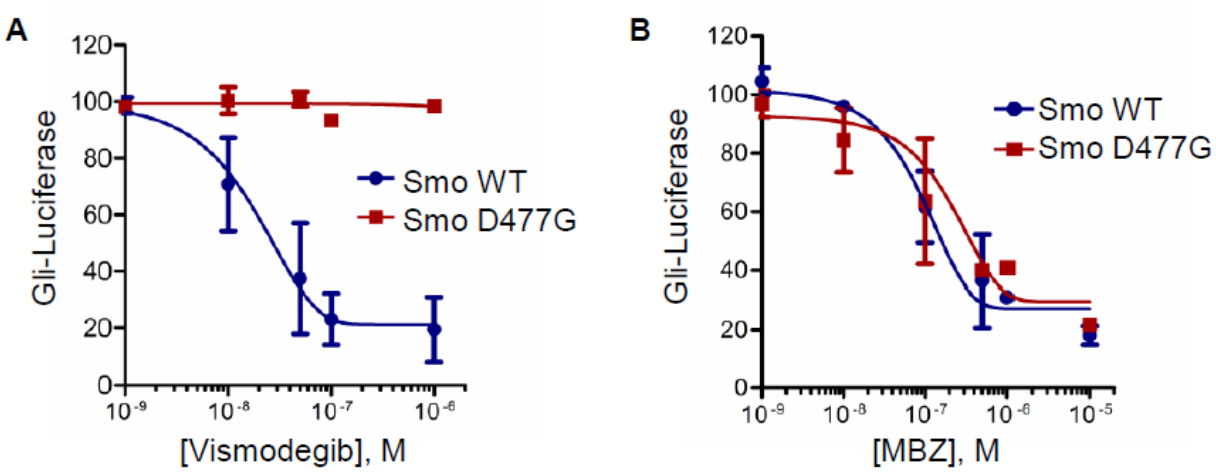

Figure 3.16. MBZ inhibits the vismodegib resistant Smo D477G mutant

Wild type *Smo* or the *Smo* D477G mutant were expressed with the Gli-luc and *renilla* luciferase reporters by co-transfection into *Smo-/-* MEFs. After 24 h, cells were treated with **(A)** vismodegib or **(B)** MBZ at the indicated concentrations, in the presence of ShhN-conditioned medium.

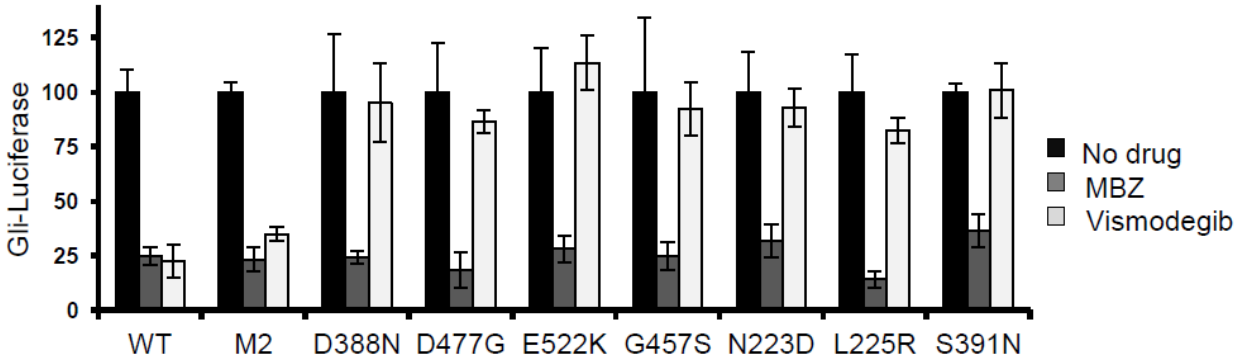

Figure 3.17. MBZ inhibits a panel of vismodegib resistant SMO mutant proteins

The effects of 1 μM MBZ and 0.2 μM vismodegib on Smo-dependent activation of the Gli-luc reporter were assessed against an expanded panel of *Smo* mutants in *Smo-/-* MEFs. WT, wild type *Smo*.

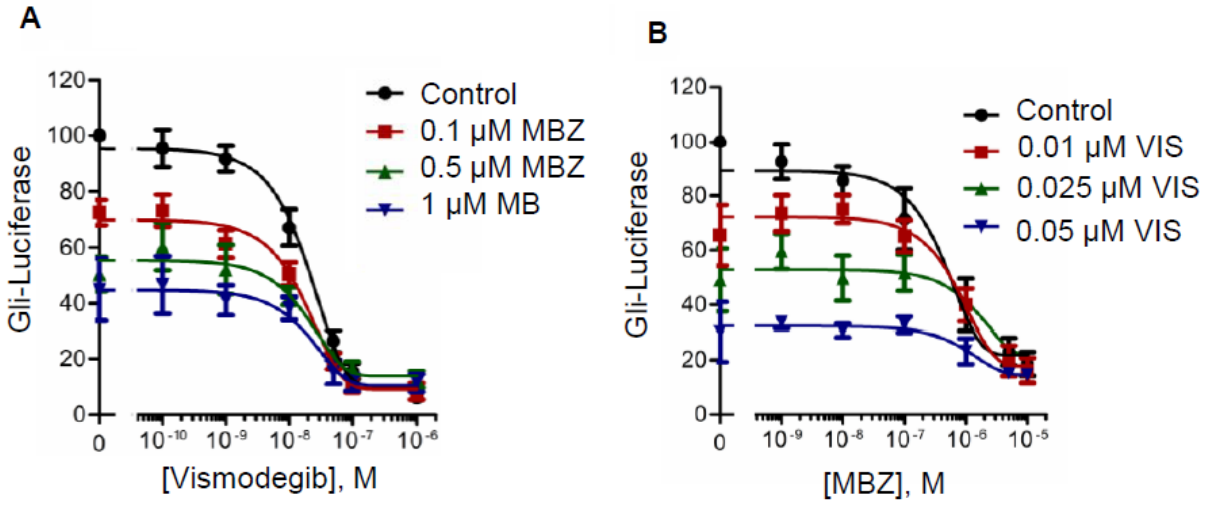

Figure 3.18. MBZ and vismodegib exert combinatorial effect on Hh

(A) The combined effects of vismodegib and MBZ on relative Gli-luc activity were tested in Shh Light2 cells under low serum conditions with supplemental ShhN-media **(B)** A modification of the experiment shown in **A**, in which MBZ was titrated into the Shh Light2 Gli-luc assay along with fixed concentrations of vismodegib.

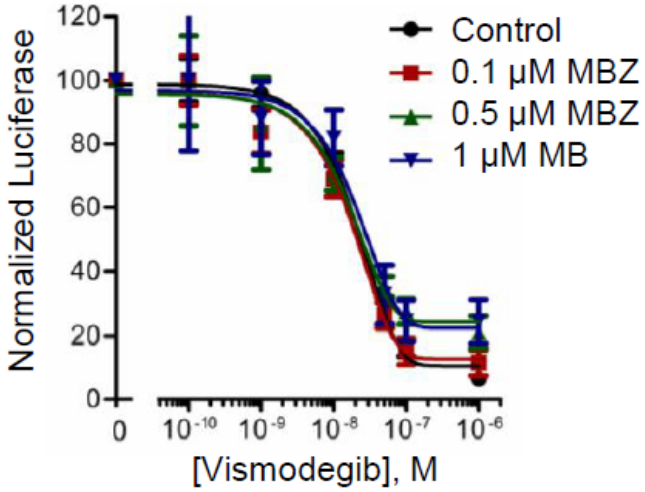

Figure 3.19 MBZ has an additive effect with vismodegib

The relative luciferase readout of **Fig 3.19.A** was normalized to 100 for each MBZ concentration, so that the curves could be superimposed. The IC_{50} of vismodegib was unchanged by addition of MBZ.

3.6. Inhibition of canonical Hh signaling by PTCH53

The canonical hedgehog pathway is negatively regulated by *PTCH1*, which suppresses SMO activity, and thereby blocks the downstream activation of the *GLI* family of transcription factors. Other *PTCH1* homologs, such as *PTCHD1*, also suppress SMO and thereby inhibit downstream Hh activation, but at reduced efficacy compared with PTCH1.

Considering the homology shared by *PTCH53* and *PTCH1*, we decided to test whether PTCH53 could suppress the canonical Hh pathway. The experiment employed the same cell line and luciferase reporter system used in Fig 3.16 and 3.17. *Smo -/-* mouse embryonic fibroblasts were transfected with a downstream luciferase reporter with eight Gli binding sites. The ability of each PTCH1 homolog (*PTCH53*, *PTCH1*, and *PTCHD1*) to suppress Gli activation was compared, by varying the ratio of each Patched protein to SMO in the transfection **(Fig 3.20)**. *PTCH53* was able to suppress canonical Gli1 activation by SMO in a dose dependent manner, to an extent that was comparable to the evolutionarily similar *PTCHD1*. However, *PTCH53* showed a reduced ability of Hh suppression relative to *PTCH1,* which exhibited similar inhibition at a 10 fold reduced concentration.

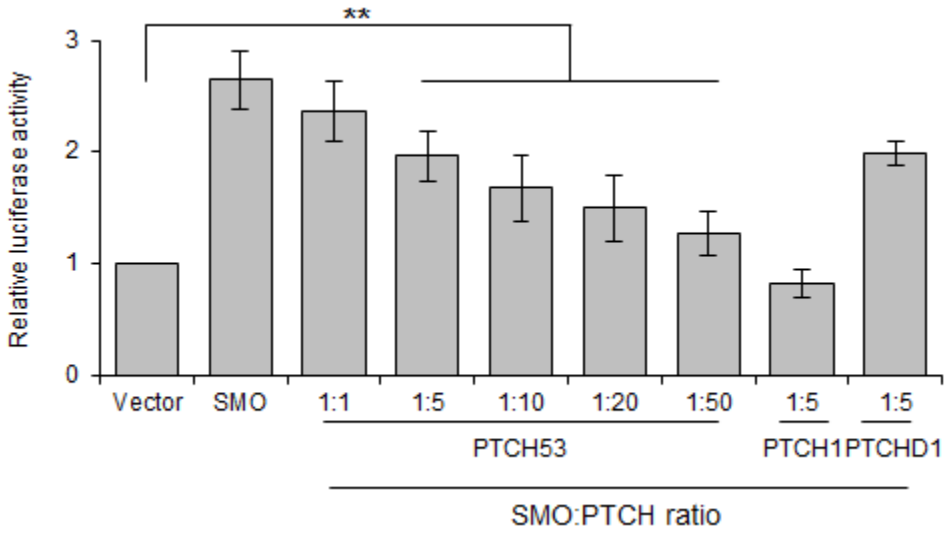

Figure 3.20. Inhibition of canonical Hh signaling by *PTCH53*

Smo-/- mouse embryonic fibroblasts were co-transfected with a *SMO* expression plasmid, a Gli-luciferase reporter and plasmids that direct the expression of *PTCH53*, *PTCH1* or *PTCHD1,* at the indicated SMO:PTCH mass ratios. Luciferase activity was assessed 72 h after transfection. *Renilla* luciferase activity was used to normalize transfection efficiency. .

3.7 Regulation of interferon-response genes by *PTCH53*

A noncanonical function of PTCH53 was suggested by the previous observation that its overexpression induced the upregulation of a set of IFN response genes **(Fig 1.2.B & 1.2.C)**. I showed that the same gene subset was upregulated in standard hTERT-RPE1 cells by IFN stimulation **(Fig. 2.21)**. Stimulation by either IFN or PTCH53 overexpression caused *MX2* transcription to be induced more than any other gene, by 1-2 log folds. *MX2* is a critical response element at inhibiting the infection of cells by human immunodeficiency virus 1 (HIV-1), vesicular stomatitis virus, and mouse herpes virus type 68 (157-160).

We used a series of p53 isogenic cell lines and cell lines with doxycycline-inducible PTCH53 shRNA to further investigate the link between *PTCH53* and induction of *MX2*. Partial knockdown of PTCH53 by doxycycline-induced shRNA caused a decrease in IFN-stimulated *MX2* transcripts **(Fig 3.22.A)** and IFN-induced MX2 protein **(Fig 3.22.B)**. *MX2* could also be induced by transfection with a 45-bp non-CpG oligomeric DNA, derived from the *Listeria monocytogenes* genome, which is a potent stimulus of the type 1 IFN response, but not by a single-stranded, non-stimulatory DNA with the same sequence **(Fig. 2.22.C)**. *PTCH53* and the p53-target gene *CDKN1A* were modestly induced after transfection with either DNA. Knockdown of *PTCH53* expression attenuated the response of *MX2* to interferon-stimulatory DNA **(Fig. 2.22.C).** We next employed isogenic colorectal cancer cells differing in functional p53 expression and therefore their ability to upregulate PTCH53. MX2 induction by IFN was significantly higher in TP53+/+ cells, compared to isogenic TP53-/- cells in both HCT116 **(Fig. 23)** and RKO **(Fig. 24)**.

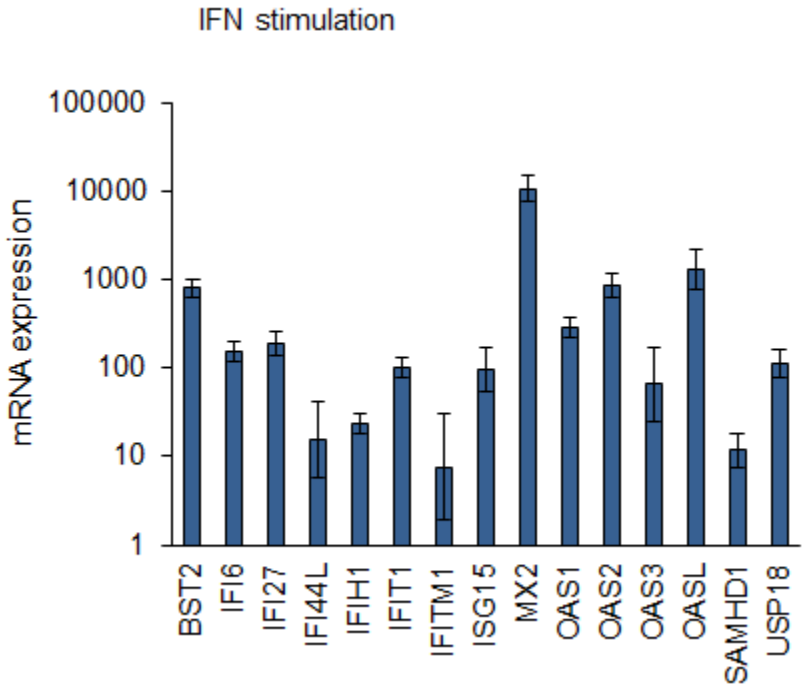

Figure 3.21. IFN induces the same panel of genes as *PTCH53* overexpression

hTERT-RPE1 cells grown in low serum conditions were treated with IFN or vehicle for 12 h. Transcripts of the 15 *PTCH53*-responsive interferon signature genes were assessed by qRT-PCR. IFN-induced expression of each gene was normalized to the uninduced expression of that gene in vehicle-treated cells.

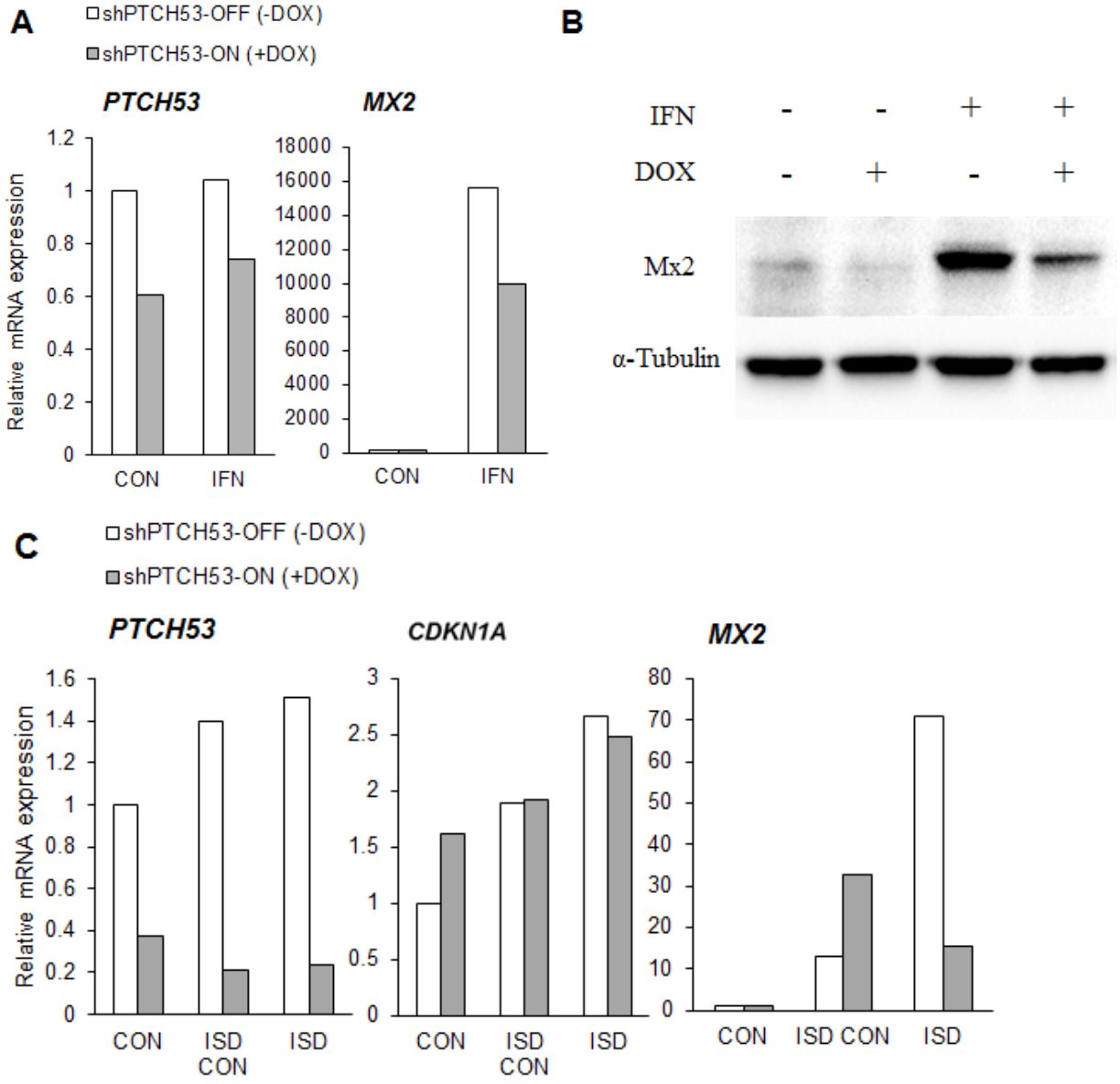

Figure 3.22. Modulation of *MX2* expression by *PTCH53* knockdown

(A) hTERT RPE1 cells with doxycycline-inducible PTCH53 shRNA were grown in low serum conditions and treated with or without doxycycline for 24 h prior to treatment with IFN or vehicle for 12 h. Transcripts were measured by qRT-PCR. **(B)** Cells were grown and treated under the same conditions as **(A)** and protein was harvested at 24 h. **(C)**

hTERT RPE1 cells with doxycycline-inducible PTCH53 shRNA, grown in low serum conditions, were treated with IFN-stimulatory DNA (ISD) or ISD control for 24 h.

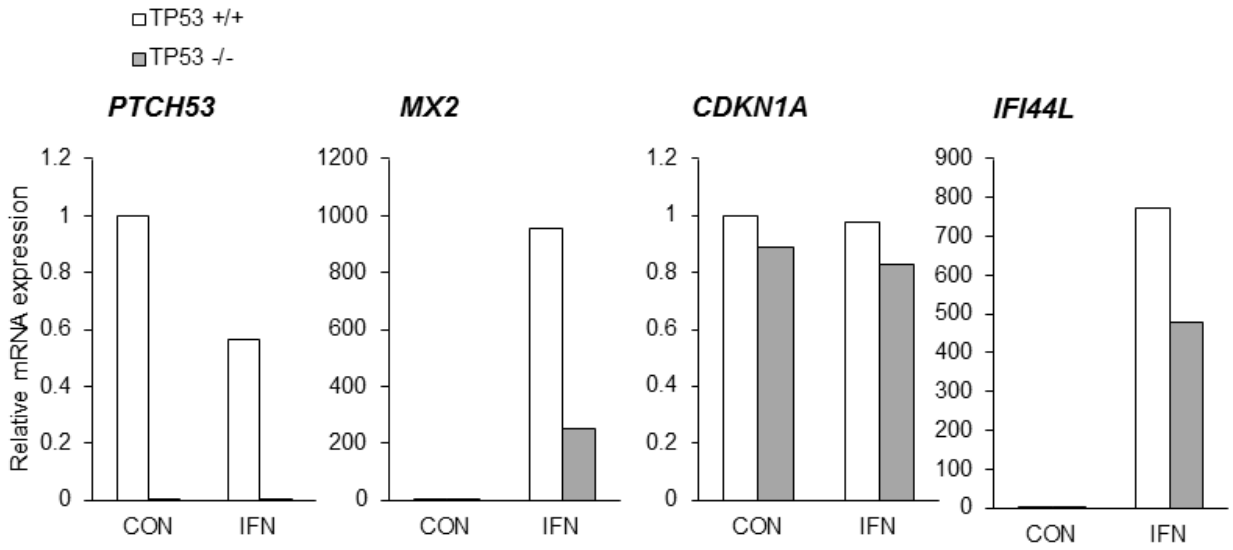

Figure 3.23 p53 dependent IFN induced *MX2* response in HCT116 cells

Isogenic *TP53* +/+ and *TP53* -/- HCT116 cells were treated with IFN or vehicle for 12 h in low serum. The indicated transcripts were assessed by qRT-PCR.

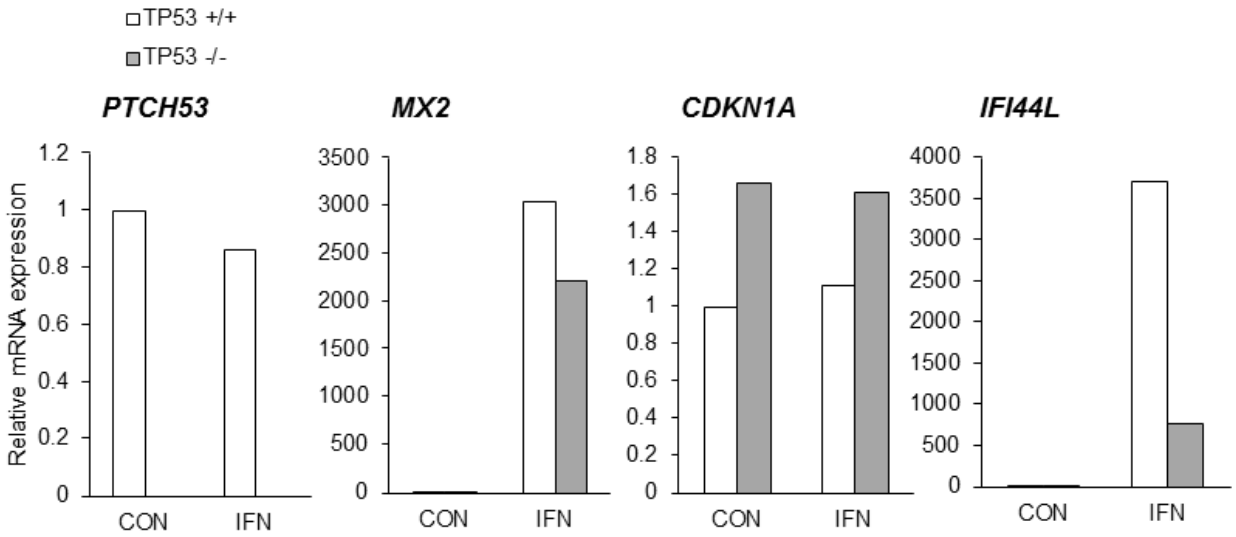

Figure 3.24 p53 dependent IFN induced response in RKO cells

Isogenic *TP53* +/+ and *TP53* -/- RKO cells were treated with IFN or vehicle for 12 h in low serum. The indicated transcripts were assessed by qRT-PCR.

Chapter 4: Discussion

4.1. Repurposing the anthelminthic mebendazole as a hedgehog inhibitor

The development of new drugs for the treatment of cancers is a time consuming and expensive process. Unanticipated toxicities at all stages of development are a major cause of failure (161). Repurposing well characterized compounds for new uses can minimize such uncertainty, save time and markedly reduce costs. There are over 4000 unique molecular entities approved worldwide for human or veterinary use (162). Exploring new indications for this rich compound library is a particularly attractive strategy to find new treatments for rare and neglected diseases, for which there are few financial incentives to justify the traditional process of commercial drug discovery. Brain tumors are relatively rare, but highly lethal. The incidence of medulloblastoma, for example, is approximately 1.5 per million in the US and the majority of these cases occur in children (163). Economic constraints and the unique vulnerability of pediatric patients are obstacles to the traditional drug discovery process. New strategies to treat such diseases will likely involve agents that are first approved for other purposes.

The low-avidity binding of MBZ to human tubulin does not evidently affect essential processes such as mitosis in normal renewing cell populations, but as we show here this interaction can inhibit the assembly of the primary cilium, a tubulin-based structure. Hh pathway components are concentrated in the primary cilium (4, 164), and mutations in murine genes necessary for cilium formation cause phenotypes consistent

with deficiencies in Hh signaling (165). In mice, primary cilia are dispensable for the growth of fibroblasts and other cell types, but essential for the ongoing proliferation of cultured medulloblastoma cells and the growth of established tumors (166). The differences in MBZ sensitivity that we observed between human medulloblastoma cells and immortalized cells (**Fig. 3.7**) are consistent with these dependencies.

The efficiency with which MBZ can inhibit the formation of the primary cilium suggests that this anti-Hh effect might account for much of its activity against brain tumors and other tumor types thus far tested. Effects on other targets may also be relevant. For example, signals arising from WNT and PDGF ligands travel through the primary cilium (3). However, the developmental abnormalities that arise in mutant mice deficient for ciliogenesis are distinct from what is observed when the WNT or PDGF-pathways are genetically altered, and most clearly overlap with those caused by Hh signaling defects (3). Beyond the primary cilium, microtubule assembly plays a fundamental role in cell division. Our results cannot rule out effects of MBZ on the mitotic spindle, but this type of antiproliferative activity is not highly specific for cancer cells. Indeed, mitotic spindle checkpoint defects that are found in many cancers have been proposed to confer relative resistance to microtubule inhibitors (167). Interestingly, MBZ-treated xenografts have been found to exhibit reduced vascularity (133), and VEGF-A has accordingly been proposed as a target of benzimidazole therapy (145). Inhibition of Hh activation potently stimulates angiogenesis by the paracrine induction of VEGF-A and other angiogenic factors (168), and could therefore account for these seemingly disparate observations.

The central role of the primary cilium in Hh pathway activation suggests that interfering with cilia formation should be an effective strategy for targeting Hh-driven tumors. The inhibitory effect of microtubule inhibitors on Hh signaling has been demonstrated by unbiased screens that have identified such agents indirectly, as inhibitors of GLI activity, or by direct inhibition of cilia formation and function (106, 169, 170). Thus far, the antimicrotubule agents identified in these screens are either highly toxic, or at early stages of characterization. Our data suggest that MBZ might represent a simple path forward for this promising therapeutic strategy.

A burgeoning body of evidence suggests that Hh signaling is involved in the initiation and/or maintenance of a large proportion of human cancers (2, 5, 6, 77). The repurposing of MBZ as an anticancer therapeutic will be guided by our rapidly growing understanding of the Hh pathway and how it contributes to tumor growth. It will be important to understand how MBZ interacts with other agents, including other Hedgehog inhibitors. In particular, the additive effect of MBZ on vismodegib that we observed *in vitro* suggests a combinatorial strategy that could potentially alleviate the untoward effects associated with vismodegib and also suppress recurrence. Clinical trials will be the next step in exploring these new possibilities.

4.2. PTCH53 as a new component of canonical and noncanonical hedgehog pathway

Our lab's identification of a novel p53 regulated tumor suppressor gene *PTCH53* provides insight into the molecular links between p53, Hh, and interferon signaling pathways. Induced expression of *PTCH53* has two consequences: inhibition of canonical Hh signaling and activation of interferon response genes. Activation of p53 has been

linked to GLI1 inhibition and PTCH53 provides a possible mechanism explaining these previously poorly understood findings (171, 172). Loss of p53 activity though mutation or deletion has been associated with activated Hh signaling and is always present in PTCH1 mutation driven tumors including medulloblastomas (66, 173). The extent of Hh regulation through suppression by functional p53 and PTCH53 in non-oncogenic cells is an area that requires further research.

PTCH53 is the first Patched homolog family to be identified as a potential regulator of an innate immune response. Whether other PTCH1 homologs share this unexpected property is unknown. p53 has been previously established as a transcriptional activator of several genes involved in the interferon response pathway including IRF5, IRF9 and ISG15, and TLR9 (174-177). Previous reports have also linked interferon stimulation to p53 overexpression and stabilization (178, 179). Our findings indicate that p53 is an upstream inducer of 15 interferon stimulated genes via *PTCH53*. Together this information proposes a possible feed forward loop that highlights the necessity of functional p53 and *PTCH53* for amplification of type 1 interferon response in the innate immune targeting of both viral infection and nascent cancer cells (180).

4.3. Future directions

Aberrant Hh pathway activation is implicated in a diverse range of cancers, many of which have limited treatment options. Therefore, preclinically identifying types of Hh driven cancers that are susceptible to MBZ treatment and identifying drugs that can be used in synergy with MBZ can optimize the next step of therapeutic strategies.

Given the tolerability and efficacy of MBZ, it would be straightforward in principle to add it as an additional component to the standard of care for many of the cancers associated with Hh activity. Unfortunately, the vast majority of Hh cancers are either not amenable to culture *in vitro* or down regulate their Hh dependence once cultured (181). Therefore, there is a lack of suitable models to test MBZ as a Hh inhibitor. It will be necessary to use Hh driven cancers with already established *in vitro* or *in vivo* models that have previously shown successful responses to vismodegib. The four models I propose to explore include basal cell carcinoma (BCC), mesothelioma, pancreatic cancer, and nevoid basal cell carcinoma (NBCC).

MBZ may be useful as a chemopreventative agent for individuals with Gorlins syndrome. Continuous treatment of low-toxicity Hh inhibitors has been proposed as a possible treatment, therefore MBZ offer an affordable, low toxicity, therapeutic option. Hh pathway has been identified as a driver of proliferation in malignant pleural mesothelioma (MPM) cells (85). Pancreatic cancer cells lines (AsPC-1, PANC-1, MIA PaCa-2) with pancreatic cancer stem markers ($CD133^+/CD44^+/CD24^+/ESA^+$) all have shown dependence on Hh pathway components.(86) Demonstrating the ability of MBZ to suppress the Hh activation in NBCC, BCC, MPM and pancreatic cancer may expand the therapeutic options for these patients.

Test MBZ efficacy against additional Hh driven cancers and syndromes..

Due to the limited models for studying BCC *in vitro*, all studies on the cancer will all be *in vivo*. Mice which develop spontaneous BCC tumors have already been engineered by collaborators. These $Ptch1^{+/-}$; $K14\text{-}Cre^{ER}$; $p53^{fl/fl}$ mice can be obtained upon request.(106) In order to ensure consistency in treatment, established BCC tumors

will be harvested from tumor bearing *Ptch1*$^{+/-}$; *K14-Cre*^{ER}; *p53*$^{fl/fl}$ mice and subcutaneously implanted as flank allografts in NOD/SCID mice (0.2 cc/mouse). 5 days post implantation; mice will begin receiving treatment in 4 randomized treatment cohorts: vehicle, MBZ (50 mg/kg), vismodegib (100mg/kg) and a combination of MBZ and vismodegib. Treatment will be administered daily by oral gavage. Flank tumor growth will be evaluated by weekly calipers measurement. Mice will be euthanized when the tumors size exceeds justifiable size in accordance with ACUC guidelines. Following sacrifice, tumors will be extracted and snap frozen. Transcriptional and translational alterations Hh pathway activity will be determined by performing qPCR and immunoblotting for Hh markers *gli1* and *ptch1*. Reduction in Hh markers levels and reduced tumor proliferation relative to vehicle would indicate successful inhibition of Hh driven growth in BCC. This experiment, if successful, should produce sufficient data to justify a clinical trial of MBZ in combination with the current standard of care, vismodegib.

To further expand the use of MBZ in Hh driven tumors, an array Hh driven malignant pleural mesothelioma cells will be tested (H27373, H245, Gardner, Gates, and H513) for inhibited growth and decreased Hh signaling in response to MBZ treatment *in vitro*. Cells will be plated and treated with increasing doses of MBZ in its range of therapeutic action (0.1-1uM) for 24 h. Following treatment, RNA will be isolated and reverse transcribed to cDNA. Transcriptional changes in the levels of *GLI1* and *PTCH1* following MBZ treatment will be assessed by qRT-PCR using vismodegib treated cells as a positive control. In conjunction, the effect of MBZ on cell proliferation will be assessed on the same array of mesothelioma cells using a standard CellTiter Blue assay. Briefly,

cells be seeded in a 96 well plate and treated with MBZ for a total of 96 hours. Absorbance readings will be obtained every 24 h to measure changes in cell proliferation following drug administration. The same Hh signaling and viability analysis performed in the mesothelioma cells will be replicated in Hh driven pancreatic cancer cell lines AsPC-1, PANC-1, MIA PaCa-2. The IC_{50} of MBZ in each cell line will be determined using CellTiter Blue and *GLI1* transcript levels will be assessed by qRT-PCR. Successfully establishing an *in vitro* model of MBZ efficacy in Hh inhibition and reduced proliferation in melanoma and pancreatic cancer will set the basis for possible future clinical trials testing MBZ effect against the cancer in patients.

A NBCC model has already been established in a $Ptch^{-/+}; p53^{-/-}$ mouse with successful spontaneous Hh driven tumors developing in over 90% of the mice (182). Once the pups are born and typed, treatment of MBZ will begin at 25 mg/kg/day. In addition to survival, the number and size of NBCC tumors presenting on the mice in each cohort will be monitored by daily caliper measurements. Whether there is a significant correlation between daily MBZ treatment and reduced NBCC emergence will enable us to determine if MBZ is a potential preventative agent and if a clinical trial should be initiated.

Increase efficacy of MBZ treatment in Hh cancer via combinatorial treatments

The effect of MBZ in combination with Hh inhibitors other than vismodegib has not been tested. We have already established a functional *in vitro* screening assay which can determine synergy. Any hits will be verified with *in vitro* and *in vivo* orthotopic models. Even if we identify combinations that are deleterious, it will be an important

clinically relevant finding to prevent any patient from ever being prescribed that combination in the future.

We will test for synergy in stages starting with compounds with the highest chances of clinical application and FDA approval to the lowest. The initial testing for combination therapy will be using and arsenic trioxide. Testing will also be completed in the seven current Phase I or II clinical trial candidates, including IPI-926, LDE225, LEQ506, PF-04449913, TAK-441, BMS833923, and LY2940680. Further testing may be completed among preclinical Hh inhibitor candidates. These compounds target a range of components in the Hh pathway including Shh, Smo, LXR, Gli, and Gli2. If any of the previous hits render a synergistic combination, we can select preclinical inhibitors that function by targeting the same Hh pathway component, to increase the probability of finding additional hits.

Based on our data relating to MBZ mechanism of Hh inhibition, knowing if a synergistic compound acts upstream or downstream of Smo would help indicate which category of inhibitor target to pursue follow up compounds. Determining synergistic combinations will likely lead to greater response in patients and decreased likelihood of resistant subclone to either treatment type.

Upon identifying the MBZ drug combination with the greatest efficacy, I will validate the combined therapy against established human Hh driven medulloblastoma model *in vitro* and *in vivo*. This will ensure that drug combination not only mechanistically inhibits the Hh pathway, but to ensure it translates to reduced proliferation in Hh driven cells. Drug combinations will be tested in our established *in vitro* assays for their effect on proliferation, survival, viability, and apoptosis by using

BrdU incorporated ELISA, clonogenic assays, CellTiter-Blue, and Hoechst 33258 staining respectively. All testing in mice will be done with 4 cohorts: vehicle, MBZ (50mg/kg), the synergist candidate alone, and combination treatment. Initial testing for synergistic or additive combination therapy will be done in a medulloblastoma allograft *in vivo* model passaged from a $Ptch^{-/+}; p53^{-/-}$ mouse background (106). The primary *in vivo* testing will be done in a flank, therefore the possibility of synergy will not be inhibited by blood brain barrier restriction and will simply be a proof of concept. Effect of the treatment on tumor growth will be evaluated by daily measurements of tumor size by caliper measurements. Upon sacrifice, tumors will be extracted and snap frozen. At the experiments completion, half of each cohort's tumors will be processed for RNA analysis in TRIzol and the other half will be preserved in formalin for subsequent processing and staining for relative expression levels of Hh signaling components. Inhibition of Hh pathways signaling will be determined by measuring levels of *Gli1* and *Ptch1* by qRT-PCR for each treatment group. Drug combinations which exhibit synergy in the flank model will subsequently be tested in the orthotopic medulloblastoma model using DAOY cerebellar implantations. This will determine if the drug combination is able to extend survival *in vivo* and will determine if the drug combination will be efficacious in this patient population.

4.4. Summary

In this dissertation, I evaluated the effects of a drug, MBZ, and a gene, *PTCH53*, on canonical Hh signaling. MBZ treatment prevented the formation of the primary cilium, decreased expression of downstream Hh pathway effectors, and decreased the proliferation and survival of human medulloblastoma cells with constitutive Hh

activation. Additionally, MBZ inhibited Hh activation in SMO mutant cells that give rise to disease recurrence, and a combination of MBZ and vismodegib achieved additive inhibition of SMO. These results support the repurposing of MBZ for use in the many types of cancers that are initiated or maintained by active Hh signaling, and suggest combinations of drugs that could facilitate the achievement of durable responses.

PTCH53 is an uncharacterized PTCH1 homolog that is activated by p53. I determined that PTCH53 can partially inhibit the canonical Hh pathway. Unexpectedly, PTCH53 could also upregulate interferon-inducible genes, in an apparent noncanonical pathway. The mechanisms by which this novel pathway function remain to be determined.

References

1. Yang L, Xie G, Fan Q, Xie J. Activation of the hedgehog-signaling pathway in human cancer and the clinical implications. Oncogene. 2010 Jan 28;29(4):469-81.

2. Barakat MT, Humke EW, Scott MP. Learning from jekyll to control hyde: Hedgehog signaling in development and cancer. Trends Mol Med. 2010 Aug;16(8):337-48.

3. Goetz SC, Anderson KV. The primary cilium: A signalling centre during vertebrate development. Nat Rev Genet. 2010 May;11(5):331-44.

4. Corbit KC, Aanstad P, Singla V, Norman AR, Stainier DY, Reiter JF. Vertebrate smoothened functions at the primary cilium. Nature. 2005 Oct 13;437(7061):1018-21.

5. Berman DM, Karhadkar SS, Maitra A, Montes De Oca R, Gerstenblith MR, Briggs K, et al. Widespread requirement for hedgehog ligand stimulation in growth of digestive tract tumours. Nature. 2003 Oct 23;425(6960):846-51.

6. Yauch RL, Gould SE, Scales SJ, Tang T, Tian H, Ahn CP, et al. A paracrine requirement for hedgehog signalling in cancer. Nature. 2008 Sep 18;455(7211):406-10.

7. Nüsslein-Volhard C, Wieschaus E. Mutations affecting segment number and polarity in drosophila. Nature. 1980;287(5785):795 <last_page> 801.

8. Riddle RD, Johnson RL, Laufer E, Tabin C. Sonic hedgehog mediates the polarizing activity of the ZPA. Cell. 1993 Dec 31;75(7):1401-16.

9. Ingham PW, McMahon AP. Hedgehog signaling in animal development: Paradigms and principles. Genes Dev. 2001 Dec 1;15(23):3059-87.

10. McMahon AP. More surprises in the hedgehog signaling pathway. Cell. 2000 Jan 21;100(2):185-8.

11. Ruiz i Altaba A. Gli proteins and hedgehog signaling: Development and cancer. Trends Genet. 1999 Oct;15(10):418-25.

12. Beachy PA, Karhadkar SS, Berman DM. Tissue repair and stem cell renewal in carcinogenesis. Nature. 2004 Nov 18;432(7015):324-31.

13. Hooper JE, Scott MP. Communicating with hedgehogs. Nat Rev Mol Cell Biol. 2005 Apr;6(4):306-17.

14. Varjosalo M, Taipale J. Hedgehog signaling. J Cell Sci. 2007 Jan 1;120(Pt 1):3-6.

15. Roessler E, Belloni E, Gaudenz K, Jay P, Berta P, Scherer SW, et al. Mutations in the human sonic hedgehog gene cause holoprosencephaly. Nat Genet. 1996;14(3):357 <last_page> 360.

16. Belloni E, Muenke M, Roessler E, Traverso G, Siegel-Bartelt J, Frumkin A, et al. Identification of sonic hedgehog as a candidate gene responsible for holoprosencephaly. Nat Genet. 1996 Nov;14(3):353-6.

17. Rubin LL, de Sauvage FJ. Targeting the hedgehog pathway in cancer. Nat Rev Drug Discov. 2006 Dec;5(12):1026-33.

18. Bastida MF, Sheth R, Ros MA. A BMP-shh negative-feedback loop restricts shh expression during limb development. Development. 2009 Nov;136(22):3779-89.

19. Bertrand N, Dahmane N. Sonic hedgehog signaling in forebrain development and its interactions with pathways that modify its effects. Trends Cell Biol. 2006 Nov;16(11):597-605.

20. Tiet TD, Alman BA. Developmental pathways in musculoskeletal neoplasia: Involvement of the indian hedgehog-parathyroid hormone-related protein pathway. Pediatr Res. 2003 Apr;53(4):539-43.

21. Karhadkar SS, Bova GS, Abdallah N, Dhara S, Gardner D, Maitra A, et al. Hedgehog signalling in prostate regeneration, neoplasia and metastasis. Nature. 2004 Oct 7;431(7009):707-12.

22. Thayer SP, di Magliano MP, Heiser PW, Nielsen CM, Roberts DJ, Lauwers GY, et al. Hedgehog is an early and late mediator of pancreatic cancer tumorigenesis. Nature. 2003 Oct 23;425(6960):851-6.

23. Porter JA, Young KE, Beachy PA. Cholesterol modification of hedgehog signaling proteins in animal development. Science. 1996 Oct 11;274(5285):255-9.

24. Micchelli CA, The I, Selva E, Mogila V, Perrimon N. Rasp, a putative transmembrane acyltransferase, is required for hedgehog signaling. Development. 2002 Feb;129(4):843-51.

25. Riobo NA, Lu K, Ai X, Haines GM, Emerson CP,Jr. Phosphoinositide 3-kinase and akt are essential for sonic hedgehog signaling. Proc Natl Acad Sci U S A. 2006 Mar 21;103(12):4505-10.

26. Ng JM, Curran T. The hedgehog's tale: Developing strategies for targeting cancer. Nat Rev Cancer. 2011 May 26;11(7):493-501.

27. Gupta S, Takebe N, Lorusso P. Targeting the hedgehog pathway in cancer. Ther Adv Med Oncol. 2010 Jul;2(4):237-50.

28. Jiang J, Hui CC. Hedgehog signaling in development and cancer. Dev Cell. 2008 Dec;15(6):801-12.

29. Charles R. Vismodegib. Clin.Cancer Res. 2012;18(12):3218-3222.

30. Ansley SJ, Badano JL, Blacque OE, Hill J, Hoskins BE, Leitch CC, et al. Basal body dysfunction is a likely cause of pleiotropic bardet-biedl syndrome. Nature. 2003 Oct 9;425(6958):628-33.

31. Adams NA, Awadein A, Toma HS. The retinal ciliopathies. Ophthalmic Genet. 2007 Sep;28(3):113-25.

32. Quarmby LM, Parker JD. Cilia and the cell cycle? J Cell Biol. 2005 Jun 6;169(5):707-10.

33. Salisbury JL. Primary cilia: Putting sensors together. Curr Biol. 2004 Sep 21;14(18):R765-7.

34. Arima T, Shibata Y, Yamamoto T. A deep-etching study of the guinea pig tracheal cilium with special reference to the ciliary transitional region. J Ultrastruct Res. 1984;89(1):34 <last_page> 41.

35. Taipale J, Cooper MK, Maiti T, Beachy PA. Patched acts catalytically to suppress the activity of smoothened. Nature. 2002 Aug 22;418(6900):892-7.

36. Hsiao YC, Tuz K, Ferland RJ. Trafficking in and to the primary cilium. Cilia. 2012 Apr 25;1(1):4,2530-1-4.

37. Rohatgi R, Milenkovic L, Scott MP. Patched1 regulates hedgehog signaling at the primary cilium. Science. 2007 Jul 20;317(5836):372-6.

38. Tran PV, Haycraft CJ, Besschetnova TY, Turbe-Doan A, Stottmann RW, Herron BJ, et al. THM1 negatively modulates mouse sonic hedgehog signal transduction and affects retrograde intraflagellar transport in cilia. Nat Genet. 2008 Apr;40(4):403-10.

39. Ferrante MI, Zullo A, Barra A, Bimonte S, Messaddeq N, Studer M, et al. Oral-facial-digital type I protein is required for primary cilia formation and left-right axis specification. Nat Genet. 2006 Jan;38(1):112-7.

40. Romio L, Fry AM, Winyard PJ, Malcolm S, Woolf AS, Feather SA. OFD1 is a centrosomal/basal body protein expressed during mesenchymal-epithelial transition in human nephrogenesis. J Am Soc Nephrol. 2004 Oct;15(10):2556-68.

41. Vierkotten J, Dildrop R, Peters T, Wang B, Ruther U. Ftm is a novel basal body protein of cilia involved in shh signalling. Development. 2007 Jul;134(14):2569-77.

42. Jenkins D. Hedgehog signalling: Emerging evidence for non-canonical pathways. Cell Signal. 2009 Jul;21(7):1023-34.

43. Brennan D, Chen X, Cheng L, Mahoney M, Riobo NA. Hedgehog signaling; noncanonical hedgehog signaling. . 2012;88:55 <last_page> 72.

44. Cayuso J, Ulloa F, Cox B, Briscoe J, Marti E. The sonic hedgehog pathway independently controls the patterning, proliferation and survival of neuroepithelial cells by regulating gli activity. Development. 2006 Feb;133(3):517-28.

45. Riobo NA, Saucy B, Dilizio C, Manning DR. Activation of heterotrimeric G proteins by smoothened. Proc Natl Acad Sci U S A. 2006 Aug 15;103(33):12607-12.

46. Chinchilla P, Xiao L, Kazanietz MG, Riobo NA. Hedgehog proteins activate pro-angiogenic responses in endothelial cells through non-canonical signaling pathways. Cell Cycle. 2010 Feb 1;9(3):570-9.

47. Thibert C, Teillet MA, Lapointe F, Mazelin L, Le Douarin NM, Mehlen P. Inhibition of neuroepithelial patched-induced apoptosis by sonic hedgehog. Science. 2003 Aug 8;301(5634):843-6.

48. Kenney AM, Rowitch DH. Sonic hedgehog promotes G(1) cyclin expression and sustained cell cycle progression in mammalian neuronal precursors. Mol Cell Biol. 2000 Dec;20(23):9055-67.

49. Kenney AM, Cole MD, Rowitch DH. Nmyc upregulation by sonic hedgehog signaling promotes proliferation in developing cerebellar granule neuron precursors. Development. 2003 Jan;130(1):15-28.

50. Barnes EA, Kong M, Ollendorff V, Donoghue DJ. Patched1 interacts with cyclin B1 to regulate cell cycle progression. EMBO J. 2001 May 1;20(9):2214-23.

51. Sasaki N, Kurisu J, Kengaku M. Sonic hedgehog signaling regulates actin cytoskeleton via Tiam1-Rac1 cascade during spine formation. Mol Cell Neurosci. 2010 Dec;45(4):335-44.

52. Pathi S, Pagan-Westphal S, Baker DP, Garber EA, Rayhorn P, Bumcrot D, et al. Comparative biological responses to human sonic, indian, and desert hedgehog. Mech Dev. 2001 Aug;106(1-2):107-17.

53. Polizio AH, Chinchilla P, Chen X, Kim S, Manning DR, Riobo NA. Heterotrimeric gi proteins link hedgehog signaling to activation of rho small GTPases to promote fibroblast migration. J Biol Chem. 2011 Jun 3;286(22):19589-96.

54. Yam PT, Langlois SD, Morin S, Charron F. Sonic hedgehog guides axons through a noncanonical, src-family-kinase-dependent signaling pathway. Neuron. 2009 May 14;62(3):349-62.

55. Bijlsma MF, Borensztajn KS, Roelink H, Peppelenbosch MP, Spek CA. Sonic hedgehog induces transcription-independent cytoskeletal rearrangement and migration regulated by arachidonate metabolites. Cell Signal. 2007 Dec;19(12):2596-604.

56. Dyer MA, Farrington SM, Mohn D, Munday JR, Baron MH. Indian hedgehog activates hematopoiesis and vasculogenesis and can respecify prospective neurectodermal cell fate in the mouse embryo. Development. 2001 May;128(10):1717-30.

57. Kobune M, Kato J, Kawano Y, Sasaki K, Uchida H, Takada K, et al. Adenoviral vector-mediated transfer of the indian hedgehog gene modulates lymphomyelopoiesis in vivo. Stem Cells. 2008 Feb;26(2):534-42.

58. Trowbridge JJ, Scott MP, Bhatia M. Hedgehog modulates cell cycle regulators in stem cells to control hematopoietic regeneration. Proc Natl Acad Sci U S A. 2006 Sep 19;103(38):14134-9.

59. Wechsler-Reya RJ, Scott MP. Control of neuronal precursor proliferation in the cerebellum by sonic hedgehog. Neuron. 1999 Jan;22(1):103-14.

60. Goodrich LV, Milenkovic L, Higgins KM, Scott MP. Altered neural cell fates and medulloblastoma in mouse patched mutants. Science. 1997 Aug 22;277(5329):1109-13.

61. Ehtesham M, Sarangi A, Valadez JG, Chanthaphaychith S, Becher MW, Abel TW, et al. Ligand-dependent activation of the hedgehog pathway in glioma progenitor cells. Oncogene. 2007 Aug 23;26(39):5752-61.

62. Clement V, Sanchez P, de Tribolet N, Radovanovic I, Ruiz i Altaba A. HEDGEHOG-GLI1 signaling regulates human glioma growth, cancer stem cell self-renewal, and tumorigenicity. Curr Biol. 2007 Jan 23;17(2):165-72.

63. Lear JT, Smith AG. Basal cell carcinoma. Postgrad Med J. 1997 Sep;73(863):538-42.

64. Unden AB, Holmberg E, Lundh-Rozell B, Stahle-Backdahl M, Zaphiropoulos PG, Toftgard R, et al. Mutations in the human homologue of drosophila patched (PTCH) in basal cell carcinomas and the gorlin syndrome: Different in vivo mechanisms of PTCH inactivation. Cancer Res. 1996 Oct 15;56(20):4562-5.

65. Wang GY, Wang J, Mancianti ML, Epstein EH,Jr. Basal cell carcinomas arise from hair follicle stem cells in Ptch1(+/-) mice. Cancer Cell. 2011 Jan 18;19(1):114-24.

66. Wetmore C, Eberhart DE, Curran T. Loss of p53 but not ARF accelerates medulloblastoma in mice heterozygous for patched. Cancer Res. 2001 Jan 15;61(2):513-6.

67. Hahn H, Wicking C, Zaphiropoulous PG, Gailani MR, Shanley S, Chidambaram A, et al. Mutations of the human homolog of drosophila patched in the nevoid basal cell carcinoma syndrome. Cell. 1996 Jun 14;85(6):841-51.

68. Hahn H, Wojnowski L, Zimmer AM, Hall J, Miller G, Zimmer A. Rhabdomyosarcomas and radiation hypersensitivity in a mouse model of gorlin syndrome. Nat Med. 1998 May;4(5):619-22.

69. Wetmore C, Eberhart DE, Curran T. The normal patched allele is expressed in medulloblastomas from mice with heterozygous germ-line mutation of patched. Cancer Res. 2000 Apr 15;60(8):2239-46.

70. Pazzaglia S, Mancuso M, Atkinson MJ, Tanori M, Rebessi S, Majo VD, et al. High incidence of medulloblastoma following X-ray-irradiation of newborn Ptc1 heterozygous mice. Oncogene. 2002 Oct 24;21(49):7580-4.

71. Massimino M, Giangaspero F, Garre ML, Gandola L, Poggi G, Biassoni V, et al. Childhood medulloblastoma. Crit Rev Oncol Hematol. 2011 Jul;79(1):65-83.

72. Schuller U, Heine VM, Mao J, Kho AT, Dillon AK, Han YG, et al. Acquisition of granule neuron precursor identity is a critical determinant of progenitor cell competence to form shh-induced medulloblastoma. Cancer Cell. 2008 Aug 12;14(2):123-34.

73. Lee Y, Miller HL, Jensen P, Hernan R, Connelly M, Wetmore C, et al. A molecular fingerprint for medulloblastoma. Cancer Res. 2003 Sep 1;63(17):5428-37.

74. Thompson MC, Fuller C, Hogg TL, Dalton J, Finkelstein D, Lau CC, et al. Genomics identifies medulloblastoma subgroups that are enriched for specific genetic alterations. J Clin Oncol. 2006 Apr 20;24(12):1924-31.

75. Kinzler KW, Bigner SH, Bigner DD, Trent JM, Law ML, O'Brien SJ, et al. Identification of an amplified, highly expressed gene in a human glioma. Science. 1987 Apr 3;236(4797):70-3.

76. Roberts WM, Douglass EC, Peiper SC, Houghton PJ, Look AT. Amplification of the gli gene in childhood sarcomas. Cancer Res. 1989 Oct 1;49(19):5407-13.

77. Watkins DN, Berman DM, Burkholder SG, Wang B, Beachy PA, Baylin SB. Hedgehog signalling within airway epithelial progenitors and in small-cell lung cancer. Nature. 2003 Mar 20;422(6929):313-7.

78. Stecca B, Mas C, Clement V, Zbinden M, Correa R, Piguet V, et al. Melanomas require HEDGEHOG-GLI signaling regulated by interactions between GLI1 and the RAS-MEK/AKT pathways. Proc Natl Acad Sci U S A. 2007 Apr 3;104(14):5895-900.

79. Bhattacharya R, Kwon J, Ali B, Wang E, Patra S, Shridhar V, et al. Role of hedgehog signaling in ovarian cancer. Clin Cancer Res. 2008 Dec 1;14(23):7659-66.

80. Simon DP, Hammer GD. Adrenocortical stem and progenitor cells: Implications for adrenocortical carcinoma. Mol Cell Endocrinol. 2012 Mar 31;351(1):2-11.

81. Teglund S, Toftgard R. Hedgehog beyond medulloblastoma and basal cell carcinoma. Biochim Biophys Acta. 2010 Apr;1805(2):181-208.

82. Lum L, Beachy PA. The hedgehog response network: Sensors, switches, and routers. Science. 2004 Jun 18;304(5678):1755-9.

83. Olive KP, Jacobetz MA, Davidson CJ, Gopinathan A, McIntyre D, Honess D, et al. Inhibition of hedgehog signaling enhances delivery of chemotherapy in a mouse model of pancreatic cancer. Science. 2009 Jun 12;324(5933):1457-61.

84. Desch P, Asslaber D, Kern D, Schnidar H, Mangelberger D, Alinger B, et al. Inhibition of GLI, but not smoothened, induces apoptosis in chronic lymphocytic leukemia cells. Oncogene. 2010 Sep 2;29(35):4885-95.

85. Jansen B, Wacheck V, Heere-Ress E, Schlagbauer-Wadl H, Hoeller C, Lucas T, et al. Chemosensitisation of malignant melanoma by BCL2 antisense therapy. Lancet. 2000;356(9243):1728-33.

86. Brahma, Singh. Junsheng, Fu. Rakesh, Srivastava. Sharmila, Shankar. Hedgehog signaling antagonist GDC-0449 (vismodegib) inhibits pancreatic cancer stem cell characteristics: Molecular mechanisms mechanisms. PLOS ONE. 2011.

87. Vogelstein B, Lane D, Levine AJ. Surfing the p53 network. Nature. 2000;408(6810):307-10.

88. el-Deiry WS, Kern SE, Pietenpol JA, Kinzler KW, Vogelstein B. Definition of a consensus binding site for p53. Nat Genet. 1992 Apr;1(1):45-9.

89. Wei CL, Wu Q, Vega VB, Chiu KP, Ng P, Zhang T, et al. A global map of p53 transcription-factor binding sites in the human genome. Cell. 2006 Jan 13;124(1):207-19.

90. Siebert JR, Cohen MMJ, Sulik KK, Shaw CM, Lemire RJ. Holoprosencephaly: Overview and atlas of cases. Plastic & Reconstructive Surgery. 1990;88(4):732.

91. Binns WJ, Shupe LF, Everett G. A congenital cyclopian-type malformation in lambs induced by maternal ingestion of a range plant, veratum californicum. Am J Vet Res. 1963;24:1164-1175.

92. Incardona J, Gafflend W, Kapur R, Roelink H. The teratogenic veratrum alkaloid cyclopamine inhibitis signal transduction. Development. 1998(125):3553-3562.

93. Taipale J, Chen JK, Cooper MK, Wang B, Mann RK, Milenkovic L, et al. Effects of oncogenic mutations in smoothened and patched can be reversed by cyclopamine. Nature. 2000 Aug 31;406(6799):1005-9.

94. Chen JK, Taipale J, Cooper MK, Beachy PA. Inhibition of hedgehog signaling by direct binding of cyclopamine to smoothened. Genes Dev. 2002 Nov 1;16(21):2743-8.

95. Meyers-Needham M, Lewis JA, Gencer S, Sentelle RD, Saddoughi SA, Clarke CJ, et al. Off-target function of the sonic hedgehog inhibitor cyclopamine in mediating apoptosis via nitric oxide-dependent neutral sphingomyelinase 2/ceramide induction. Mol Cancer Ther. 2012 May;11(5):1092-102.

96. Amakye D, Jagani Z, Dorsch M. Unraveling the therapeutic potential of the hedgehog pathway in cancer. Nat Med. 2013 Nov;19(11):1410-22.

97. Robarge KD, Brunton SA, Castanedo GM, Cui Y, Dina MS, Goldsmith R, et al. GDC-0449-a potent inhibitor of the hedgehog pathway. Bioorg Med Chem Lett. 2009 Oct 1;19(19):5576-81.

98. Low JA, de Sauvage FJ. Clinical experience with hedgehog pathway inhibitors. J Clin Oncol. 2010 Dec 20;28(36):5321-6.

99. LoRusso PM, Rudin CM, Reddy JC, Tibes R, Weiss GJ, Borad MJ, et al. Phase I trial of hedgehog pathway inhibitor vismodegib (GDC-0449) in patients with refractory, locally advanced or metastatic solid tumors. Clin Cancer Res. 2011 Apr 15;17(8):2502-11.

100. Von Hoff DD, LoRusso PM, Rudin CM, Reddy JC, Yauch RL, Tibes R, et al. Inhibition of the hedgehog pathway in advanced basal-cell carcinoma. N Engl J Med. 2009 Sep 17;361(12):1164-72.

101. Berlin J, Bendell JC, Hart LL, Firdaus I, Gore I, Hermann RC, et al. A randomized phase II trial of vismodegib versus placebo with FOLFOX or FOLFIRI and bevacizumab in patients with previously untreated metastatic colorectal cancer. Clin Cancer Res. 2013 Jan 1;19(1):258-67.

102. Rudin CM, Hann CL, Laterra J, Yauch RL, Callahan CA, Fu L, et al. Treatment of medulloblastoma with hedgehog pathway inhibitor GDC-0449. New England Journal of Medicine. 2009;361(12):1173-1178.

103. Yauch RL, Dijkgraaf GJ, Alicke B, Januario T, Ahn CP, Holcomb T, et al. Smoothened mutation confers resistance to a hedgehog pathway inhibitor in medulloblastoma. Science. 2009 Oct 23;326(5952):572-4.

104. Kim J, Aftab BT, Tang JY, Kim D, Lee AH, Rezaee M, et al. Itraconazole and arsenic trioxide inhibit hedgehog pathway activation and tumor growth associated with acquired resistance to smoothened antagonists. Cancer Cell. 2013 Jan 14;23(1):23-34.

105. DiMasi JA, Feldman L, Seckler A, Wilson A. Trends in risks associated with new drug development: Success rates for investigational drugs. Clin Pharmacol Ther. 2010 Mar;87(3):272-7.

106. Kim J, Tang JY, Gong R, Kim J, Lee JJ, Clemons KV, et al. Itraconazole, a commonly used antifungal that inhibits hedgehog pathway activity and cancer growth. Cancer Cell. 2010 Apr 13;17(4):388-99.

107. Georgopapadakou NH, Walsh TJ. Antifungal agents: Chemotherapeutic targets and immunologic strategies. Antimicrob Agents Chemother. 1996 Feb;40(2):279-91.

108. Lamb DC, Kelly DE, Waterman MR, Stromstedt M, Rozman D, Kelly SL. Characteristics of the heterologously expressed human lanosterol 14alpha-demethylase (other names: P45014DM, CYP51, P45051) and inhibition of the purified human and candida albicans CYP51 with azole antifungal agents. Yeast. 1999 Jun 30;15(9):755-63.

109. Stevens DA. Managing fungal infections in the 21st century: Focus on itraconazole. Drugs. 2001;61:1-56.

110. Romer JT, Kimura H, Magdaleno S, Sasai K, Fuller C, Baines H, et al. Suppression of the shh pathway using a small molecule inhibitor eliminates medulloblastoma in Ptc1(+/-)p53(-/-) mice. Cancer Cell. 2004 Sep;6(3):229-40.

111. Berman DM, Karhadkar SS, Hallahan AR, Pritchard JI, Eberhart CG, Watkins DN, et al. Medulloblastoma growth inhibition by hedgehog pathway blockade. Science. 2002 Aug 30;297(5586):1559-61.

112. Song X, Hu X, Lü S, Gao L, Chen L, Yang J, et al. Incorporation of arsenic trioxide in induction therapy improves survival of patients with newly diagnosed acute promyelocytic leukaemia. Eur J Haematol. 2014:n/a <last_page> n/a.

113. Kinjo K, Kizaki M, Muto A, Fukuchi Y, Umezawa A, Yamato K, et al. Arsenic trioxide (As2O3)-induced apoptosis and differentiation in retinoic acid-resistant acute promyelocytic leukemia model in hGM-CSF-producing transgenic SCID mice. Leukemia. 2000 Mar;14(3):431-8.

114. Beauchamp EM, Ringer L, Bulut G, Sajwan KP, Hall MD, Lee Y, et al. Arsenic trioxide inhibits human cancer cell growth and tumor development in mice by blocking hedgehog/GLI pathway. J Clin Invest. 2011;121(1):148 <last_page> 160.

115. Montesinos P, Sanz MA. The differentiation syndrome in patients with acute promyelocytic leukemia: Experience of the pethema group and review of the literature. Mediterr J Hematol Infect Dis. 2011;3(1):e2011059.

116. Zhou J. Arsenic trioxide: An ancient drug revived. Chin Med J. 2012;125(19):3556-60.

117. Kritharis A, Bradley TP, Budman DR. The evolving use of arsenic in pharmacotherapy of malignant disease. Ann Hematol. 2013;92(6):719.

118. Rudin CM, Brahmer JR, Juergens RA, Hann CL, Ettinger DS, Sebree R, et al. Phase 2 study of pemetrexed and itraconazole as second-line therapy for metastatic nonsquamous non-small-cell lung cancer. J Thorac Oncol. 2013 May;8(5):619-23.

119. Antonarakis ES, Heath EI, Smith DC, Rathkopf D, Blackford AL, Danila DC, et al. Repurposing itraconazole as a treatment for advanced prostate cancer: A noncomparative randomized phase II trial in men with metastatic castration-resistant prostate cancer. Oncologist. 2013;18(2):163-73.

120. Xie J, Bartels CM, Barton SW, Gu D. Targeting hedgehog signaling in cancer: Research and clinical developments. Onco Targets Ther. 2013 Oct 10;6:1425-35.

121. Kamal SM, El Sayed Khalifa K. Immune modulation by helminthic infections: Worms and viral infections. Parasite Immunol. 2006 Oct;28(10):483-96.

122. Velíka J, Baliharováb V, Fink-Gremmelsc J, Bullc S, Lamkaa J, Skálováb L. Benzimidazole drugs and modulation of biotransformation enzymes. Research in Veterinary Science. 2004;76(2):95-108.

123. Borgers M, De Nollin S, De Brabander M, Thienpont D. Influence of the anthelmintic mebendazole on microtubules and intracellular organelle movement in nematode intestinal cells.. American Journal of Veterinary Research. 1975;8:1153-1166.

124. Friedman PA, Platzer EG. Interaction of anthelmintic benzimidazoles and benzimidazole derivatives with bovine brain tubulin. Biochim Biophys Acta. 1978 Dec 18;544(3):605-14.

125. Russell GJ, Gill JH, Lacey E. Binding of [3H]benzimidazole carbamates to mammalian brain tubulin and the mechanism of selective toxicity of the benzimidazole anthelmintics. Biochem.Pharmacol. 1992;43(5):1095-100.

126. Ammann R, Fleiner-Hoffmann A, Grimm F, Eckert J. Long-term mebendazole therapy may be parasitocidal in alveolar echinococcosis. Journal of Hepatology. 1998(29):994-998.

127. Bryceson AD, Woestenborghs R, Michiels M, van den Bossche H. Bioavailability and tolerability of mebendazole in patients with inoperable hydatid disease. Trans R Soc Trop Med Hyg. 1982;76(4):563-4.

128. Braithwaite PA, Roberts MS, Allan RJ, Watson TR. Clinical pharmacokinetics of high dose mebendazole in patients treated for cystic hydatid disease. Eur J Clin Pharmacol. 1982;22(2):161-9.

129. Dayan AD. **Albendazole, mebendazole and praziquantel. review of non-clinical toxicity and pharmacokinetics**. Acta Tropica. 2003;86(2-3):141-159.

130. Bekhti A. Serum concentrations of mebendazole in patients with hydatid disease. Int J Clin Pharmacol Ther Toxicol. 1985 Dec;23(12):633-41.

131. Munst GJ, Karlaganis G, Bircher J. Plasma concentrations of mebendazole during treatment of echinococcosis. European journal of clinical pharmacology. 1980;17(5):375.

132. Bai RY, Staedtke V, Aprhys CM, Gallia GL, Riggins GJ. Antiparasitic mebendazole shows survival benefit in 2 preclinical models of glioblastoma multiforme. Neuro Oncol. 2011 Sep;13(9):974-82.

133. Mukhopadhyay T, Sasaki J, Ramesh R, Roth JA. Mebendazole elicits a potent antitumor effect on human cancer cell lines both in vitro and in vivo. Clin Cancer Res. 2002 Sep;8(9):2963-9.

134. Sasaki J, Ramesh R, Chada S, Gomyo Y, Roth JA, Mukhopadhyay T. The anthelmintic drug mebendazole induces mitotic arrest and apoptosis by depolymerizing tubulin in non-small cell lung cancer cells. Mol Cancer Ther. 2002 Nov;1(13):1201-9.

135. Martarelli D, Pompei P, Baldi C, Mazzoni G. Mebendazole inhibits growth of human adrenocortical carcinoma cell lines implanted in nude mice. Cancer Chemother Pharmacol. 2008 Apr;61(5):809-17.

136. Doudican N, Rodriguez A, Osman I, Orlow SJ. Mebendazole induces apoptosis via bcl-2 inactivation in chemoresistant melanoma cells. Mol Cancer Res. 2008 Aug;6(8):1308-15.

137. Doudican NA, Byron SA, Pollock PM, Orlow SJ. XIAP downregulation accompanies mebendazole growth inhibition in melanoma xenografts. Anticancer Drugs. 2013;24(2):181 <last_page> 188.

138. Nygren P, Fryknas M, Agerup B, Larsson R. Repositioning of the anthelmintic drug mebendazole for the treatment for colon cancer. J Cancer Res Clin Oncol. 2013 Dec;139(12):2133-40.

139. Dakshanamurthy S, Issa NT, Assefnia S, Seshasayee A, Peters OJ, Madhavan S, et al. Predicting new indications for approved drugs using a proteochemometric method. J Med Chem. 2012 Aug 9;55(15):6832-48.

140. Martarelli D, Pompei P, Baldi C, Mazzoni G. Mebendazole inhibits growth of human adrenocortical carcinoma cell lines implanted in nude mice. Cancer Chemother Pharmacol. 2008 Apr;61(5):809-17.

141. Dobrosotskaya IY, Hammer GD, Schteingart DE, Maturen KE, Worden FP. Mebendazole monotherapy and long-term disease control in metastatic adrenocortical carcinoma. Endocr Pract. 2011 May-Jun;17(3):e59-62.

142. Nygren P, Larsson R. Drug repositioning from bench to bedside: Tumour remission by the antihelmintic drug mebendazole in refractory metastatic colon cancer. Acta Oncol. 2013 Oct 28.

143. Monje M, Mitra SS, Freret ME, Raveh TB, Kim J, Masek M, et al. Hedgehog-responsive candidate cell of origin for diffuse intrinsic pontine glioma. Proc Natl Acad Sci U S A. 2011 Mar 15;108(11):4453-8.

144. Gruber Filbin M, Dabral SK, Pazyra-Murphy MF, Ramkissoon S, Kung AL, Pak E, et al. Coordinate activation of shh and PI3K signaling in PTEN-deficient glioblastoma: New therapeutic opportunities. Nat Med. 2013 Nov;19(11):1518-23.

145. Pourgholami MH, Yan Cai Z, Lu Y, Wang L, Morris DL. Albendazole: A potent inhibitor of vascular endothelial growth factor and malignant ascites formation in OVCAR-3 tumor-bearing nude mice. Clin Cancer Res. 2006 Mar 15;12(6):1928-35.

146. Papadopoulos N, Nicolaides NC, Liu B, Parsons R, Lengauer C, Palombo F, et al. Mutations of GTBP in genetically unstable cells. Science. 1995 Jun 30;268(5219):1915-7.

147. Low WC, Wang C, Pan Y, Huang XY, Chen JK, Wang B. The decoupling of smoothened from galphai proteins has little effect on Gli3 protein processing and hedgehog-regulated chick neural tube patterning. Dev Biol. 2008 Sep 1;321(1):188-96.

148. Roessle E, Ermilov AN, Grange DK, Wang A, Grachtchouk M, Dlugosz AA, et al. A previously unidentified amino-terminal domain regulates transcriptional activity of wild-type and disease-associated human GLI2. Hum Mol Genet. 2005 Aug 1;14(15):2181-8.

149. Noor A, Whibley A, Marshall CR, Gianakopoulos PJ, Piton A, Carson AR, et al. Disruption at the PTCHD1 locus on Xp22.11 in autism spectrum disorder and intellectual disability. Science Translational Medicine. 2010;2(49).

150. Shimokawa T, Svärd J, Heby-Henricson K, Teglund S, Toftgård R, Zaphiropoulos PG. Distinct roles of first exon variants of the tumor-suppressor Patched1 in hedgehog signaling. Oncogene. 2007;26(34):4889-4896.

151. Sharma N, Kosan ZA, Stallworth JE, Berbari NF, Yoder BK. Soluble levels of cytosolic tubulin regulate ciliary length control. Mol Biol Cell. 2011 Mar 15;22(6):806-16.

152. Jin H, White SR, Shida T, Schulz S, Aguiar M, Gygi SP, et al. The conserved bardet-biedl syndrome proteins assemble a coat that traffics membrane proteins to cilia. Cell. 2010 Jun 25;141(7):1208-19.

153. Jacobs VL, Valdes PA, Hickey WF, De Leo JA. Current review of in vivo GBM rodent models: Emphasis on the CNS-1 tumour model. ASN Neuro. 2011 Aug 3;3(3):e00063.

154. Triscott J, Lee C, Foster C, Manoranjan B, Pambid MR, Berns R, et al. Personalizing the treatment of pediatric medulloblastoma: Polo-like kinase 1 as a molecular target in high-risk children. Cancer Res. 2013 Nov 7.

155. Northcott PA, Korshunov A, Pfister SM, Taylor MD. The clinical implications of medulloblastoma subgroups. Nat Rev Neurol. 2012 May 8.

156. Martinelli DC, Fan CM. Gas1 extends the range of hedgehog action by facilitating its signaling. Genes Dev. 2007 May 15;21(10):1231-43.

157. Goujon C, Moncorge O, Bauby H, Doyle T, Ward CC, Schaller T, et al. Human MX2 is an interferon-induced post-entry inhibitor of HIV-1 infection. Nature. 2013 Oct 24;502(7472):559-62.

158. Kane M, Yadav SS, Bitzegeio J, Kutluay SB, Zang T, Wilson SJ, et al. MX2 is an interferon-induced inhibitor of HIV-1 infection. Nature. 2013 Oct 24;502(7472):563-6.

159. Liu Z, Pan Q, Ding S, Qian J, Xu F, Zhou J, et al. The interferon-inducible MxB protein inhibits HIV-1 infection. Cell Host Microbe. 2013 Oct 16;14(4):398-410.

160. Liu SY, Sanchez DJ, Aliyari R, Lu S, Cheng G. Systematic identification of type I and type II interferon-induced antiviral factors. Proc Natl Acad Sci U S A. 2012 Mar 13;109(11):4239-44.

161. Kola I, Landis J. Can the pharmaceutical industry reduce attrition rates? Nat Rev Drug Discov. 2004 Aug;3(8):711-5.

162. Huang R, Southall N, Wang Y, Yasgar A, Shinn P, Jadhav A, et al. The NCGC pharmaceutical collection: A comprehensive resource of clinically approved drugs enabling repurposing and chemical genomics. Sci Transl Med. 2011 Apr 27;3(80):80ps16.

163. Smoll NR, Drummond KJ. The incidence of medulloblastomas and primitive neurectodermal tumours in adults and children. J Clin Neurosci. 2012 Nov;19(11):1541-4.

164. Rohatgi R, Milenkovic L, Scott MP. Patched1 regulates hedgehog signaling at the primary cilium. Science. 2007 Jul20;317(5836):372-6.

165. Huangfu D, Anderson KV. Cilia and hedgehog responsiveness in the mouse. Proc Natl Acad Sci U S A. 2005 Aug 9;102(32):11325-30.

166. Barakat MT, Humke EW, Scott MP. Kif3a is necessary for initiation and maintenance of medulloblastoma. Carcinogenesis. 2013 Jun;34(6):1382-92.

167. Weaver BA, Cleveland DW. Decoding the links between mitosis, cancer, and chemotherapy: The mitotic checkpoint, adaptation, and cell death. Cancer Cell. 2005 Jul;8(1):7-12.

168. Chen W, Tang T, Eastham-Anderson J, Dunlap D, Alicke B, Nannini M, et al. Canonical hedgehog signaling augments tumor angiogenesis by induction of VEGF-A in stromal perivascular cells. Proc Natl Acad Sci U S A. 2011 May 19.

169. Hyman JM, Firestone AJ, Heine VM, Zhao Y, Ocasio CA, Han K, et al. Small-molecule inhibitors reveal multiple strategies for hedgehog pathway blockade. Proc Natl Acad Sci U S A. 2009 Aug 18;106(33):14132-7.

170. Wu VM, Chen SC, Arkin MR, Reiter JF. Small molecule inhibitors of smoothened ciliary localization and ciliogenesis. Proc Natl Acad Sci U S A. 2012 Aug 21;109(34):13644-9.

171. Stecca B, Ruiz i Altaba A. A GLI1-p53 inhibitory loop controls neural stem cell and tumour cell numbers. EMBO J. 2009 Mar 18;28(6):663-76.

172. Jones DT, Jager N, Kool M, Zichner T, Hutter B, Sultan M, et al. Dissecting the genomic complexity underlying medulloblastoma. Nature. 2012 Aug 2;488(7409):100-5.

173. Vogelstein B, Papadopoulos N, Velculescu VE, Zhou S, Diaz LA,Jr, Kinzler KW. Cancer genome landscapes. Science. 2013 Mar 29;339(6127):1546-58.

174. Hummer BT, Li XL, Hassel BA. Role for p53 in gene induction by double-stranded RNA. J Virol. 2001 Aug;75(16):7774-7.

175. Mori T, Anazawa Y, Iiizumi M, Fukuda S, Nakamura Y, Arakawa H. Identification of the interferon regulatory factor 5 gene (IRF-5) as a direct target for p53. Oncogene. 2002;21(18):2914-8.

176. Taura M, Eguma A, Suico MA, Shuto T, Koga T, Komatsu K, et al. p53 regulates toll-like receptor 3 expression and function in human epithelial cell lines. Mol Cell Biol. 2008 Nov;28(21):6557-67.

177. Rivas C, Aaronson SA, Munoz-Fontela C. Dual role of p53 in innate antiviral immunity. Viruses. 2010;2(1):298 <last_page> 313.

178. Munoz-Fontela C, Macip S, Martinez-Sobrido L, Brown L, Ashour J, Garcia-Sastre A, et al. Transcriptional role of p53 in interferon-mediated antiviral immunity. J Exp Med. 2008 Aug 4;205(8):1929-38.

179. Takaoka A, Hayakawa S, Yanai H, Stoiber D, Negishi H, Kikuchi H, et al. Integration of interferon-alpha/beta signalling to p53 responses in tumour suppression and antiviral defence. Nature. 2003 Jul 31;424(6948):516-23.

180. Platanias LC. Mechanisms of type-I- and type-II-interferon-mediated signalling. Nat Rev Immunol. 2005 May;5(5):375-86.

181. Stecca B, Ruiz I Altaba A. Context-dependent regulation of the GLI code in cancer by HEDGEHOG and non-HEDGEHOG signals. J Mol Cell Biol. 2010 Apr;2(2):84-95.

182. Hahn H, Wicking C, Zaphiropoulous PG, Gailani MR, Shanley S, Chidambaram A, et al. Mutations of the human homolog of drosophila patched in the nevoid basal cell carcinoma syndrome. Cell. 1996 Jun 14;85(6):841-51.

Curriculum Vitae

Andrew R. Larsen

Larsen@jhmi.edu
Work (410) 502-8135 **Cell** (978) 460-1576

Work Address
1550 Orleans St, Rm 462
Baltimore MD, 21231

Home Address
103 W Monument St, Apt 2a
Baltimore MD, 21231

EDUCATION

Johns Hopkins University School of Medicine, Baltimore, MD
- Graduated March, 2014
- Ph.D. in Cellular and Molecular Medicine
- Advisor: Fred Bunz M.D., Ph.D.
- Thesis: Targeting Canonical and Noncanoncial Signaling Pathways in Cancer

Skidmore College, Saratoga Springs, NY
- Graduated May, 2009
- Major: Chemistry with a biochemistry concentration
- Minor: Business
- Thesis: Synthesis and Purification of 5-oxo-dodecanoyl Analogs

RESEARCH EXPERIENCE

Graduate Researcher
Johns Hopkins University School of Medicine, Baltimore MD
Department of Radiation Oncology, 2012-2014
- Doctoral Thesis work with Fred Bunz, M.D., Ph.D.
- Studying the noncanonical function of a novel *Patched* homolog and repurposing mebendazole as a hedgehog inhibitor in cancer.

Department of Neurobiology, 2010-2011
- Research with Russell L. Margolis, M.D.
- Defining the role of inherited NPAS3 mutations in schizophrenia.

Research Assistant
Skidmore College, Saratoga Springs, NY
Chemistry Department, 2008-2009
- Advisor: Rajesh Nagarajan, Ph.D.
- Synthesis and purification of novel LasI synthase inhibitors to suppress *P. aeruginosa* biofilm formation.

Research Intern
Genzyme Pharmaceuticals, Waltham, MA
Process Chemistry Department of Drug Discovery & Development Division, 2008

- Advisor: Richard Silva, Ph.D.
- Optimizing synthesis of Renvela and preliminary synthesis mechanisms for a novel liver cancer drug.

PUBLICATIONS

Larsen, AR, Bai, RY, Chung, JH, Riggins, GJ, Bunz, F. Repurposing the anthelmintic mebendazole as a hedgehog inhibitor. *Cancer Research* (In review, 2014)

Chung, JH, **Larsen, AR**, Chen, E, Bunz, F. A human *Patched* gene regulated by p53 stimulates expression of the antiviral factor MX2. *Science Signaling* (Submitted, 2014)

HONORS & AWARDS

Incentive Mentoring Program, Baltimore, MD

- Mentoring family of the month, 2014
- Head of house leadership award, 2013
- Adaptability in leadership award, 2012

Skidmore College, Saratoga Springs, NY

- Dean's list: 2006-2009
- Graduated Periclean Society Member and Cum Laude

PATENTS

Larsen, AR, Riggins, GJ, Bunz, F. "Repurposing mebendazole as a hedgehog inhibitor." Submitted to Johns Hopkins University Tech Transfer **2014.**

Chung JH, **Larsen, AR**, Bunz, F. "Induction of Antiviral Immunity by a DNA Damage-responsive Signaling Protein" Submitted to Johns Hopkins University Tech Transfer **2014.**

COMMUNITY INVOVLEMENT

Incentive Mentoring Program, Baltimore, MD

Mentor, 2009-2014

- Helped tutor disadvantaged inner city high school students

Head of House, 2011-2014

- Coordinated a team of mentors for tutoring, SAT and college prep
- Raised GPA from 0.67 to 3.0

PROFESSIONAL MEMBERSHIPS

American Chemistry Society (2008-Present)
American Academy of Arts and Sciences (2009-Present)
Society for Neuroscience (2010-Present)